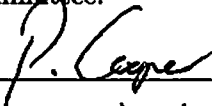


THE FORMATION AND REACTIONS OF OXIDANTS IN WATER ICE

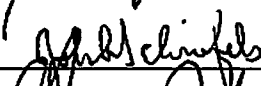
by

Nhut H. Do  
A Dissertation  
Submitted to the  
Graduate Faculty  
of  
George Mason University  
In Partial fulfillment of  
The Requirements for the Degree  
of  
Doctor of Philosophy  
Chemistry and Biochemistry

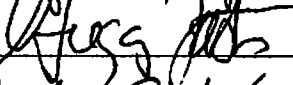
Committee:

  
\_\_\_\_\_

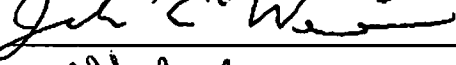
Dr. Paul Cooper, Dissertation Director

  
\_\_\_\_\_

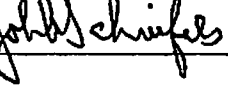
Dr. John Schreifels, Committee Member

  
\_\_\_\_\_

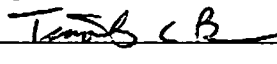
Dr. Gregory Foster, Committee Member

  
\_\_\_\_\_

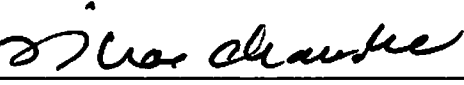
Dr. Joseph Weingartner, Committee Member

  
\_\_\_\_\_

Dr. John Schreifels, Department Chair

  
\_\_\_\_\_

Dr. Timothy L. Born, Associate Dean for  
Student and Academic Affairs, College of  
Science

  
\_\_\_\_\_

Dr. Vikas Chandhoke, Dean, College of  
Science

Date: April 12, 2013

Spring Semester 2013  
George Mason University  
Fairfax, VA

The Formation and Reactions of Oxidants in Water Ice

A dissertation submitted in partial fulfillment of the requirements for the degree of  
Doctor of Philosophy at George Mason University

By

Nhut H. Do  
Bachelor of Science  
Virginia Commonwealth University, 2007

Director: Dr. Paul Cooper, Professor  
Department of Chemistry and Biochemistry

Spring Semester 2013  
George Mason University  
Fairfax, VA

Copyright © 2013 by Nhut H. Do  
All Rights Reserved

## Dedication

I dedicate this dissertation to my parents and my grandparents.

## Acknowledgments

I would like to thank Dr. Cooper for his help and making my Ph.D. project possible. I also would like to thank the committee for their time: Dr. Schreifels, Dr. Foster, Dr. Weingartner. Finally, I would like to thank my friends and family for their encouragements over the years to push me forward.

# Table of Contents

	Page
List of Tables . . . . .	vi
List of Figures . . . . .	vii
Abstract . . . . .	ix
1 Introduction . . . . .	1
1.1 Radiation Processes . . . . .	2
1.2 Related Work . . . . .	5
1.2.1 Studies of Water Ice . . . . .	5
1.2.2 H <sub>2</sub> O <sub>2</sub> . . . . .	8
1.2.3 O <sub>2</sub> & O <sub>3</sub> . . . . .	12
1.3 The Outer Solar System . . . . .	15
2 Experimental . . . . .	22
3 Results . . . . .	28
3.1 Data . . . . .	28
3.2 Discussions . . . . .	48
3.2.1 Ice Experiments . . . . .	48
3.2.2 O Atom Experiments . . . . .	48
3.2.3 Similar Experiments Different Results . . . . .	49
3.2.4 OH . . . . .	53
3.2.5 HO <sub>2</sub> and HO <sub>3</sub> . . . . .	54
3.2.6 O Atom . . . . .	57
3.2.7 Impact of this Work . . . . .	59
3.3 Conclusion . . . . .	60
Bibliography . . . . .	62

## List of Tables

Table		Page
1.1	Physical parameters of the Galilean satellites [NASA Fact Sheet]. . . . .	16
2.1	Summary of radiation and temperatures in irradiated ice experiments. . . .	23
3.1	Band assignments ( $\text{cm}^{-1}$ ) of $(\text{H}_2\text{O})_n$ in matrix isolated $\text{H}_2\text{O}:\text{Ne}$ (1:100) compare to literature. nrm = non-rotating monomer. . . . .	32
3.2	Column densities and thickness of $\text{H}_2\text{O}:\text{He}$ and $\text{H}_2\text{O}:\text{Ne}$ 1:100 ice. *Concentration below detection limit of instrument. . . . .	38

## List of Figures

Figure	Page
1.1 UV reflectance of H <sub>2</sub> O <sub>2</sub> on Europa compared with laboratory diffuse reflectance measurements indicating between 0.13 and 0.16% H <sub>2</sub> O <sub>2</sub> by number relative to water [14]. . . . .	11
1.2 IR absorbance spectra of O <sub>3</sub> isotopologues with increasing radiation dose [30].	14
1.3 Galilean satellites. From left to right: Io, Europa, Ganymede, and Callisto. [NASA Photojournal] . . . . .	15
1.4 Image of Europa taken by the Galileo orbiter. [NASA Photojournal] . . . .	17
1.5 Volcanic plume on Io. Imaged by New Horizons. [NASA Photojournal] . . .	18
1.6 Image of a cratered Callisto. [NASA Photojournal] . . . . .	20
2.1 Schematic of typical traditional experiments. . . . .	22
2.2 Deposition of radiowave discharged H <sub>2</sub> O/Rare Gas mixture. . . . .	25
2.3 Actual deposition setup. 1. Tesla coil 2. Water mixtures flow through glass tube where discharge occurs 3. 360 degrees rotatable sample holder 90 degree facing inlet port. . . . .	25
2.4 Stainless steel gas manifold and two 1L glass bulbs used for mixing and storing water and rare gas mixtures. . . . .	26
2.5 Diagram of stainless steel vacuum system. . . . .	27
3.1 IR spectrum of matrix isolated H <sub>2</sub> O:Ne (1:100) at 6K (top) and after warming to 20K (bottom). . . . .	29
3.2 1750 to 1550 cm <sup>-1</sup> matrix isolated H <sub>2</sub> O:Ne at 6K without discharge (bottom) and with discharge (top). PA = proton acceptor, PD = proton donor. . . .	30
3.3 4100 to 2900 cm <sup>-1</sup> matrix isolated H <sub>2</sub> O:Ne at 6K without discharge (bottom) and with discharge (top). . . . .	31
3.4 OH and HO <sub>2</sub> in H <sub>2</sub> O:Ar 1:100 matrix. . . . .	33
3.5 Triplet O atom in H <sub>2</sub> O:Ar 1:100 matrix. . . . .	34
3.6 OH absorption in the UV. . . . .	35

3.7	Helium and H <sub>2</sub> O mixtures 1:100 ratios deposited from 20K to 80K in 10K interval. . . . .	36
3.8	Neon and H <sub>2</sub> O mixtures 1:100 ratios deposited from 20K to 80K in 10K interval. . . . .	37
3.9	Spectra of deposited water at 2 torr for pure water (solid line), discharged pure water (dotted line), and discharged H <sub>2</sub> O:He 1:10 (dashed line) all at 6K. . . . .	39
3.10	Deposition at 30K and warmed up to 150K in 30K interval. . . . .	40
3.11	Dependence of normalized H <sub>2</sub> O <sub>2</sub> absorption band area upon warming of ice samples deposited at 30 K (red squares) and 60 K (black circles). . . . .	41
3.12	TPD (Mass 32) of ice deposited at 30K, 60K, 90K, and 120K. . . . .	42
3.13	UV spectra of solid O <sub>2</sub> . . . . .	43
3.14	Co-deposition of O <sub>2</sub> :He (discharged) and H <sub>2</sub> O:He in 1:100 ratio at various temperatures. . . . .	44
3.15	Band area of H <sub>2</sub> O <sub>2</sub> vs. deposition temperature. . . . .	45
3.16	(a) O <sub>2</sub> :Ar discharged deposition at 6K, (b) H <sub>2</sub> O:Ar deposition on top of a, (c) layered warmed to 25K, (d) warmed to 40K. . . . .	46
3.17	4000 to 2400 cm <sup>-1</sup> spectra of (a) O <sub>2</sub> :Ar discharged deposition at 6K, (b) H <sub>2</sub> O:Ar deposition on top of a, (c) layered warmed to 25K, (d) warmed to 40K. . . . .	47

## Abstract

THE FORMATION AND REACTIONS OF OXIDANTS IN WATER ICE

Nhut H. Do, PhD

George Mason University, 2013

Dissertation Director: Dr. Paul Cooper

This dissertation investigates the chemistry in water ice of radical species, such as OH and O, produced in radio-frequency discharge. This novel method of studying such reactive species in water ice is a departure from traditional laboratory methods that have been used for more than thirty years. The main difference is that the radicals are produced in the gas phase and deposited concurrently as the ice film grows as opposed to being produced in-situ via photolysis or radiolysis of the ice. Like the traditional method, oxidants such as hydrogen peroxide ( $\text{H}_2\text{O}_2$ ), oxygen ( $\text{O}_2$ ) and ozone ( $\text{O}_3$ ) are produced and detected by infrared (IR), ultra-violet (UV), or mass spectrometry. The new method I have developed allows for the quantification of the initial amounts of radical species deposited in the ice which is otherwise impossible with traditional methods. This new feature is important to determining the role of radical species in the formation of oxidants relevant to surfaces on outer solar system bodies.

There are conflicting data in the literature on the radiation induced chemistry of water ice such as the formation pathways of  $\text{H}_2\text{O}_2$  and  $\text{O}_2$ , or the detection of oxidants on icy satellites in the outer solar system. The main goal of this dissertation is to provide experimental evidence and chemical analysis to the role of precursors (OH, O-atom) leading to the formation of oxidants, mainly  $\text{H}_2\text{O}_2$ . This experimental method is based upon the matrix isolated technique used in the past to study reactive species and weak molecular bonds such as water-hydroxyl ( $\text{H}_2\text{O}$ -HO) complexes in rare gas matrices. The difference in the present experiments is that the deposition of the discharged gas mixture is set at a temperature at which the rare gas does not stick to form matrices. Instead, an ice is made containing radical species. The results not only show that this method can produce the same oxidants found in traditionally irradiated experiments, but in certain cases with much higher  $\text{H}_2\text{O}_2$  abundances. Thermal experiments also showed that  $\text{H}_2\text{O}_2$  and  $\text{O}_3$  are stable up to 150K when samples were deposited at 30K and warmed to 150K. The results are potentially important for understanding the chemical evolution of icy objects in the solar system (and universe).

## Chapter 1: Introduction

The laboratory study of the radiation effects on water ice has been an interesting topic since the discovery of water ice in the outer solar system and their exposure to high flux of energetic radiation. The detection of oxidants such as molecular oxygen ( $O_2$ ) [13, 134] and hydrogen peroxide ( $H_2O_2$ ) [14] trapped on the icy surface of the Galilean satellites and Saturn's ring [61, 141, 151] prompted experimental studies [28, 42, 87, 94, 104, 140] to trace the precursors responsible for this chemistry. Although we have a good understanding of the incident radiation that causes the chemistry, there are not enough experimental data on the role of radicals that are responsible for formation of oxidants. Studying the formation pathways and chemical evolution is important to current modeling efforts such as the processes responsible for the production of oxygen ions within Saturn's ring [88] or the astro-biological relevance of the possible transport of oxidants to a subsurface ocean on Europa [23]. In the past, traditional laboratory experiments provided spectral data which help interpret observations by space telescopes (Hubble) and fly-by missions such as Pioneers, Voyagers, Galileo and most recently the Cassini mission; these efforts have resulted in identification of oxidants such as hydrogen peroxide ( $H_2O_2$ ) on Europa [14] and molecular oxygen ( $O_2$ ) on Ganymede [13] which helped us understand more about the chemistry of outer solar system bodies. However, there are conflicting data on the chemical pathways leading to the formation of hydrogen peroxide ( $H_2O_2$ ), molecular oxygen ( $O_2$ ), and ozone ( $O_3$ ). With an emphasis on radiation chemistry and by employing a new laboratory approach, this dissertation aims to provide experimental evidence that will contribute to this ongoing discussion.

Traditional laboratory studies of radiation effects on ice have involved forming ices by vapor deposition, followed by irradiation of the ice and observations of the processed sample

by IR or UV and sometimes mass spectrometry for sputtering/desorption experiments. This is what I shall call the deposit-irradiate-analyze method. The problem with this method is that radicals are made *in-situ* and are often present in small quantities. Additionally, the OH radical cannot be measured in the IR due to the present of the broad water band at  $\sim 3300\text{ cm}^{-1}$  where it also absorbs in the IR. This is undesirable as the amount of radicals cannot be quantified in order to compare to the amount of oxidants produced. In the current method, radicals are produced in a discharge and deposit concurrently with water and an inert rare gas mixture onto a cold substrate. Depending on the substrate temperature, two different types of ices can be formed. At temperatures below 6K, matrix isolated ice can be formed. For temperatures above the rare gas sublimation point, water ice samples are formed. Using the combined data from the matrix and the ice experiments provides the ability to detect and track the reactive intermediates responsible for the oxidation chemistry.

In this research, I investigate the formation of oxidants by using this novel method and make chemical comparisons to traditional methods. The main question that will be answered will be what is the role of radicals in the formation of  $\text{H}_2\text{O}_2$  and how can we use this method to better understand the reactivity of radicals such as OH,  $\text{HO}_2$  and O atoms. Recently, there was a journal published on the detection of OH radicals in water ice [158] in which the technique is similar to this research, however, their interpretation of the data is incorrect and I addressed this in detail in the discussion section of this dissertation.

## 1.1 Radiation Processes

Outer solar system bodies and even interstellar grains are covered in water ice and have been subject to intense radiation bombardment from energetic ions or UV photons for millions of years. The composition of the surface and atmosphere of these airless bodies are believed to be shaped by the surrounding radiation field. Through the study of radiation chemistry of ices we hope to learn about the compositions and properties of these icy surfaces and most importantly the origin and evolution of satellites and ring systems. In these environments, radiolysis and photolysis are prevalent and dominates the chemistry of not just water ice but

also hydrated materials (e.g.  $\text{MgSO}_4\text{H}_2\text{O}$ ). Radiolysis and photolysis refer to the chemistry that follows the excitation of atoms and molecules by energetic particles, electrons, or ultraviolet (UV) photons. Radiolysis involves charged particles ( $\text{S}^{n+}$ ,  $\text{O}^{n+}$ ,  $\text{He}^{+..}$ ), protons and electrons where photolysis is the excitation by UV photons. Radiolysis and photolysis are likely responsible for the production of tholins [21, 117] in Titan's atmosphere.

Most satellites or moons orbiting Jupiter and Saturn are covered in water ice [33, 83, 113]. The lack of a substantial atmosphere results in radiolysis of the icy surface; however, there is also a constant exchange of molecules between the solid phase and gas phase. Understanding the chemistry that occurs on the surfaces of these satellites is important to understanding the surface composition and their tenuous atmospheres. Average surface temperatures on the Galilean satellites ranges from 103K (-170C) to 118K (-155C) compare to Earth at 288K (15C) and Mars at 210K (-63C) [NASA Fact Sheet]. These extreme low temperatures allow the trapping of volatiles in the ice surface that can be observed by UV or IR spectra. The Galilean and Saturnian systems interacts with their icy satellites via radiation bombardments of the surface which is facilitated by the great extent of their magnetospheres [116, 123, 150, 154]. The first fly-by mission to Jupiter was made by the Pioneer 10, which discovered an unusually high plasma density within the magnetosphere [93]. An estimate of the average surface energy flux from magnetospheric irradiation of the Galilean satellites is around  $10^{11} \text{ keV cm}^{-2} \text{ s}^{-1}$  [24]. This is higher than the energy flux of Earth's Van Allen radiation belt ( $\sim 10^8 \text{ keV cm}^{-2} \text{ s}^{-1}$ ). Particles and electrons trapped in these magnetospheres are further accelerated by mechanisms such as radial diffusions [81] and wave accelerations [51]. Without an atmosphere to protect itself, these satellites are subject to intense plasma bombardments which lead to chemical changes, erosions and sputtering of particles from the surface. Sputtering come from energetic heavy particle bombardments. Endogenic sources of plasma ( $\text{H}^+$ ,  $\text{He}^+$ ,  $\text{e}^-$ ) originates from the parent planet or the nearby satellites via sputtering, but exogenic sources come from solar winds or cosmic rays. Processes such as sublimation, sputtering, desorption, and cryo-volcanic activities are ways atoms and molecules are ejected from the ice surface [25, 33, 71, 126].

Due to relatively weak gravitational fields, small molecules (such as  $\text{H}_2$ ) with enough escape energy will be lost into space. However, heavier molecules can be trapped within the tenuous atmosphere and can re-deposit back to the ice surface. These molecules could be a mixture of  $\text{O}_2$ ,  $\text{H}_2\text{O}_2$ , OH radicals, and  $\text{H}_2\text{O}$ . This process of re-deposition or resurfacing may play an important role in the production and trapping of oxygen ( $\text{O}_2$ ), hydrogen peroxide ( $\text{H}_2\text{O}_2$ ), and ozone ( $\text{O}_3$ ), and thus determine surface composition at icy bodies throughout the outer solar system.

Sputtering is the process of ejecting atoms or molecules from a surface by plasma or micrometeorite bombardments [45]. Heavy ions can sputter neutrals 100s of km into space [131]. A recent study shows heavy-ion ( $\text{He}^{2+}$ ,  $\text{O}^{7+}$ ) bombardments from coronal mass ejection on the lunar surface increases the concentrations of exospheric ions [73]. Sputtering has been proposed as a process of enriching the surface of the Saturnian satellites with water over time by the ejection of ammonia ( $\text{NH}_3$ ) [80]. This process is important to understanding the compositions of plasma in the vicinity of a satellite where it is the cause of surface erosions [57]. Sputtered particles or ejecta can be resurfaced, form an exosphere, or escape into space. Sputtering may be one of the processes responsible for some of the observed neutral clouds in the outer solar system such as Europa's sodium [10, 59] and oxygen exospheres [56]. Resurfacing processes may play an important role in the transport of sulfur atoms from the surface of Io to other Galilean satellites [138]. Important information about the surface can be extracted since sputtered materials can be analyzed by a spacecraft's instrument [68, 115].

Sputtering effects on water ice has been studied since the 1970s. In the laboratory, sputtering is studied by exposing a sample to a source of energetic heavy ions and the sputtered material is directly measured by secondary ion mass spectrometry (SIMS). Lanzerotti and Brown [79] first looked at the sputtering rates of water by radiation at the Galilean moons, they showed that water sputtering by energetic protons was an efficient process which was later predicted [63] to be a main contributor to the oxygen atmosphere on Europa [56, 125]. An  $\text{O}_2$  exosphere was discovered on Europa soon after with an estimated column density

of about  $1.5 \times 10^{15} \text{ cm}^{-2}$  [46]. Sputtering on Europa is a result of bombardments by keV sulfur ( $S^{n+}$ ) and oxygen ( $O^{n+}$ ) ions. The yield was estimated to be about 200-300 ejected  $H_2O$  molecules per incident ion and approximately 20-30% of the sputtered  $H_2O$  may escape permanently from the surface while the bulk of materials are resurfaced [63]. In addition to  $H_2O$ , volatiles such as  $H_2$  and  $O_2$  are also ejected.  $H_2$  is lost to space due to its low molecular weight and binding energy resulting in an oxidized surface [62].  $O_2$  does not stick for long on the surface as the temperature is above its sublimation point in a vacuum, therefore, make up the majority of the gas phase molecules in the atmosphere. In comparison, an  $SO_2$  rich surface sputtering yield is 400-600 molecule per incident ion and the ejecta are mainly  $SO_2$ ,  $SO$ , and  $O_2$  [63, 64].

In theory, there are three types of sputtering in irradiated ice. Knock-on sputtering is when atoms are "knocked" from their sites forming defects in the bulk material if the atoms are on the surface then ejection would follow. In electronic sputtering, neutrals are being ejected. Chemical sputtering is when molecules that are ejected are products of irradiation that have low binding energy to the ice (i.e.  $H_2$ ). Chemical sputtering promotes diffusion of volatiles and efficiently removes it from the ice lattice as shown in sputtering experiments [80].

## 1.2 Related Work

In this section, a background on experimental work will be given for the basic understanding and current challenges. It is dedicated to past and current laboratory efforts in regards to the study of precursors ( $OH$ ,  $O$ ) and oxidants ( $H_2O_2$ ,  $O_2$ ,  $O_3$ ) formations in water ice.

### 1.2.1 Studies of Water Ice

Since the 1950s, reactive species have been studied by the matrix isolation technique which was proposed by Pimentel et al. [153]. The present study of radiation effects in ice is an extension of this method. In fact, this dissertation was motivated by the study of  $H_2O \cdot HO$

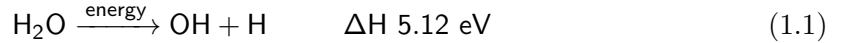
complexes in argon matrices [27]. In matrix isolation spectroscopy, reactive species (RS) - produced by various methods - are deposited alongside a rare gas (RG) in dilute mixtures (<1:100 RS:RG) onto a transparent or reflective substrate with temperatures usually below 10K. Subsequently, these reactive species are trapped in inert matrices for spectroscopic determinations. Nitrogen, neon, argon, krypton, xenon, and para-hydrogen are some of the common inert gases used for the matrix [17, 20, 112]. Pyrolysis, photolysis, laser ablation, and microwave discharge are a few methods that have been used in producing radicals for matrix isolation experiments [90]. The experiments in this paper uses the radio-frequency discharge method, which is a low-cost and effective way of producing radicals (OH, O) from water vapor. Infrared (IR) spectroscopy is the most popular tool used for determination of the reactive species. Spectroscopically, molecules behave differently in the solid phase than in the gas phase and there is even a greater effect when it is isolated in inert matrices. For example, matrix isolated water will form aggregates or become cyclic  $((\text{H}_2\text{O})_n$  where n can be as high as 6) [49]. OH radicals are known to complex with water in argon matrices. Spectral shifting due to site effects is a common feature associated with matrix isolation spectroscopy. In the gas phase, the IR absorptions for the symmetric ( $\nu_1$ ) and anti-symmetric stretch ( $\nu_3$ ) are  $3657 \text{ cm}^{-1}$  and  $3756 \text{ cm}^{-1}$  [128] respectively, however, they are red-shifted to  $3627 \text{ cm}^{-1}$  and  $3725 \text{ cm}^{-1}$  in nitrogen matrices [144]. The matrix isolation method by microwave discharge is ideal for studying the interaction of radicals, intermediates or weak complexes by limiting the mobility and reactivity by confining them inside inert cages. However, it does not provide much information about their reactivity or formation pathways.

Some of the first irradiated water ice experiments were done in the 1960s [99, 129, 139] where crystalline ice samples were pulse irradiated with electrons produced by a Van de Graaf generator. Solvated electrons ( $e^-_s$ ) were observed in the visible at 670 nm, this feature was refer to as e-vis. The role of the solvated electrons are unknown and difficult to observe since its' lifetime is in the picosecond timescale. This work was followed by pulse photolysis of water ice where the flash was produced by Xe or Hg-Xe lamps [41], however,

e-vis was not observed. The implications for this difference are not known. These early experiments provided valuable insights on the radiation chemistry of water ice.

Recent experimental efforts focus on the pathways of oxidant formations, such as molecular oxygen ( $\text{O}_2$ ) [104, 127, 130] and hydrogen peroxide ( $\text{H}_2\text{O}_2$ ) [42, 53, 94] motivated by the discovery of oxidants on Galilean and Saturnian satellites. Cooper et al. [28] recently showed that irradiation of  $\text{H}_2\text{O} + \text{O}_2$  ices produces  $\text{O}_3$ ,  $\text{H}_2\text{O}_2$ , and  $\text{HO}_2$  which is an important model to the production of oxidants in icy satellite surfaces. As a result of the discovery of  $\text{H}_2\text{O}_2$  on Europa, Moore and Hudson [94] provided experimental data on  $\text{H}_2\text{O}_2$  formation from ion irradiated water ice. Most recently, O atoms were implicated in the formation of  $\text{O}_2$  in water ice from ozone isotopologue experiments [30] which was an important extension to the previous work before it [65, 110, 140].

In the laboratory, ion irradiation of water ice films has been shown to produce  $\text{O}_2$  [104, 127, 130], and  $\text{H}_2\text{O}_2$  [42, 85, 94, 157]. The production of these molecules is made by *in-situ* irradiation of thin films of  $\text{H}_2\text{O}$  ice. The process occur by energetic dissociation of water via,



and



where molecular hydrogen [4] were observed but lost from the surface in vacuum. The main problem with irradiated ice experiments is the branching ratio for the two equations above is unknown. This creates difficulty in determining the formation pathways. It was mainly believed that the very reactive hydroxyl radicals combine to form hydrogen peroxide,



however, there may be more than one pathways as singlet O atoms can also be produce

from the discharge. Singlet O atoms can react via,



$\text{H}_2\text{O}_2$  is a precursor of  $\text{O}_2$  [130, 157] since reaction 1.4 can reverse producing O atoms and they can combine to form  $\text{O}_2$  by



In addition,  $\text{O}_2$  is a precursor to ozone since this reaction can occur between triplet O atoms and  $\text{O}_2$ ,



This relationship between  $\text{H}_2\text{O}_2$ ,  $\text{O}_2$ , and  $\text{O}_3$  make some interesting chemistry in irradiated water ice as they also pertain to icy surface of outer solar system bodies. There are some unsolved problems regarding the  $\text{O}_2$  present on the surface of the Galilean satellites [13, 134, 135] and  $\text{O}_3$  on Ganymede [101], Rhea, and Dione [103]. Solid  $\text{O}_2$  is unstable in a vacuum at temperatures above 30K, and so it is still unclear how the  $\text{O}_2$  is present on the surface of these satellites [13]. Experimental studies have shown that  $\text{O}_2$  can be trapped in micro-porous water ice below 110K [91] and the trapping is enhanced with ion irradiation of the porous ice [127]. However, the astronomical data has yet to be replicated by laboratory measurements. Water ice is almost ubiquitous to the outer solar system and these processes are likely occurring everywhere there is a presence of radiation and water, and is not unique to the Galilean satellites.

### 1.2.2 $\text{H}_2\text{O}_2$

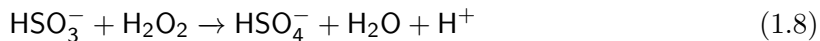
$\text{H}_2\text{O}_2$  is an important molecule here on Earth and observed in space on the surface of Europa [14] and even interstellar grains [37]. It is a highly reactive oxidizer and is known as a sterilization agent.  $\text{H}_2\text{O}_2$  decomposes in the presence of many metals/reducing agents such

as steel and iron. This is the main problem in temperature desorption studies as  $\text{H}_2\text{O}_2$  decomposes once in contact with the stainless steel vacuum chamber. Mass spectrometry will most likely contribute to  $\text{O}_2$  or  $\text{H}_2\text{O}$  mass reading. In Earth's atmosphere, the only known source of  $\text{H}_2\text{O}_2$  come from the second order reaction of two hydroperoxy radicals [31, 136] ( $\text{HO}_2$ ),



Kinetic studies shows the rate of reaction to increase with pressure but decreases with temperature [74] and the presence of water vapor positively influences the reaction rates [47, 84]. This is important to tropospheric chemistry where water vapor, OH and  $\text{HO}_2$  are dominant species. In addition to photolysis,  $\text{H}_2\text{O}_2$  formation also occur via atmospheric electrical discharges; both  $\text{H}_2\text{O}_2$  and  $\text{O}_3$  have been observed in higher concentrations after thunderstorms below the tree canopy of a forest [7].

$\text{H}_2\text{O}_2$  influence weather on Earth by acid rain production and dissolution from the atmosphere into sinks such as hydrometeors and the ocean [149]. Acid rain formation occurs via the oxidation of sulfur (IV) to sulfur (VI) which transform  $\text{HSO}_3^-$  to  $\text{HSO}_4^-$  [108]



This could have a negative impact on the pH of the oceans. Trace amounts of  $\text{H}_2\text{O}_2$  measured in ice cores have provide key information about the temperature, accumulation, and composition of current and past atmospheres [70]. In fact, concentrations of  $\text{H}_2\text{O}_2$  decreases with depth in Greenland and Antarctica and overall have increased by 50% over the past 200 years [132].

$\text{HO}_x$  (OH and  $\text{HO}_2$ ) are important radicals for  $\text{H}_2\text{O}_2$  chemistry. They're important oxidizers in the atmosphere and responsible for the photochemical destruction of ozone [43, 89, 133, 148, 152] and hydrogen peroxide [3, 75, 76, 143]. Both destruction processes also serve as a temporary reservoir for  $\text{HO}_2$ ,



$\text{HO}_2$  can also come from the reactions of isoprene and the burning of biomass, while OH primary formation pathway is from the photolysis of ozone [137] ( $\lambda < 340$  nm),



$\text{HO}_x$  are important radicals in gas phase chemistry.  $\text{H}_2\text{O}\cdot\text{HO}$  complex and free OH radicals have been isolated in argon matrix experiments in the IR at  $3450\text{ cm}^{-1}$  [1] and  $3550\text{ cm}^{-1}$  [27], respectively. The UV absorption of OH in ice is at  $0.28\text{ }\mu\text{m}$  [139]. Spectroscopic identification of OH is well known, the spectral difference between the gas and solid phase is the shift in positions of the OH absorption band. Complexation of OH and water in argon matrix isolation experiments shows three main absorption peaks at 3452, 3428, and  $3442\text{ cm}^{-1}$  in agreement with theoretical values [27]. OH can be produced by the photolysis of  $\text{H}_2\text{O}_2$  ice [22], this is an important process in atmospheric chemistry where radicals has an effect on the oxidative environment. Photolysis of  $\text{H}_2\text{O}$  ice produces not only  $\text{H}_2\text{O}_2$  but also OH and  $\text{HO}_2$  [40]. However,  $\text{HO}_2$  is seen in  $\text{H}_2\text{O}$  photolysis only with  $\text{O}_2$  present [58].

Following the detection of  $\text{H}_2\text{O}_2$  at  $3.50\text{ }\mu\text{m}$  ( $2857\text{ cm}^{-1}$ ) by Galileo's infrared mapping spectrometer (NIMS) on the surface of Europa and the estimated surface concentration of  $\text{H}_2\text{O}_2$  relative to  $\text{H}_2\text{O}$  was 0.13 %, the structure of  $\text{H}_2\text{O}_2$  was experimentally identified to be in the form of dispersed  $\text{H}_2\text{O}_2\cdot 2\text{H}_2\text{O}$  trimers [86]. So far, hydrogen peroxide has only been detected on Europa. It's been shown in the laboratory that water ice exposed to a radiation source (UV, protons, or electrons) produces  $\text{H}_2\text{O}_2$ . From this we might conclude

that  $\text{H}_2\text{O}_2$  should be present on any water ice surface satellites within the Jovian and/or Saturnian systems—where energetic particles are abundant. However, the detection of  $\text{H}_2\text{O}_2$  seem to be difficult due to weak absorption bands and is more complicated by presence of impurities in the ice which is a source of spectral interference. The problem currently faced is detecting  $\text{H}_2\text{O}_2$  on satellites beyond Europa. Ganymede and Callisto are further away from Jupiter and do not get as much magnetospheric radiation as Europa. Therefore, the  $\text{H}_2\text{O}_2$  yield would be significantly less and harder to detect remotely. The same case can be made for Saturnian satellites. Although we assume that  $\text{H}_2\text{O}_2$  exists on these satellites, current observations have not detect  $\text{H}_2\text{O}_2$  beyond Europa.

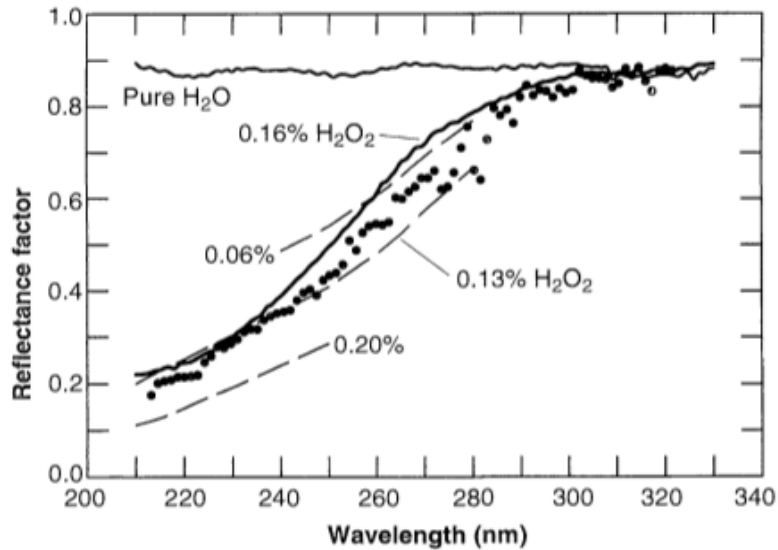


Figure 1.1: UV reflectance of  $\text{H}_2\text{O}_2$  on Europa compared with laboratory diffuse reflectance measurements indicating between 0.13 and 0.16%  $\text{H}_2\text{O}_2$  by number relative to water [14].

Many relevant experimental studies of irradiated  $\text{H}_2\text{O}$  has been performed in the last decade with the purposes of quantifying and detecting  $\text{H}_2\text{O}_2$  on icy satellites. However, there are differences in the data as the production of  $\text{H}_2\text{O}_2$  is hard to replicate by the current method because of sensitivity to temperature and radiation sources. Moore and Hudson [94] first observed  $\text{H}_2\text{O}_2$  in proton ( $\text{H}^+$ , 0.8 MeV) irradiated pure  $\text{H}_2\text{O}$  ice at 16K. However, it was

only seen at 80K when O<sub>2</sub> or CO<sub>2</sub> is present in the ice film. They suggest that there are complex ice mixtures on Europa. In fact, Europa's surface is not only water ice but is considered to have impurities such as SO<sub>2</sub>, and CO<sub>2</sub> [48, 78]. Gomis et al. [42] showed that proton (H<sup>+</sup>, C<sup>+</sup>, N<sup>+</sup>, O<sup>+</sup>, and Ar<sup>+</sup>) irradiation of pure water ice produced H<sub>2</sub>O<sub>2</sub> at both 16K and at 80K. Gomis et al. irradiated a sample thicker than Moore & Hudson's with particle energy of 30 keV as opposed to 800 keV. They suggested that the particle formation rates of hydrogen peroxide produced by H<sup>+</sup> irradiation are much lower than the heaviest ions and the H<sub>2</sub>O<sub>2</sub> could not be detected by Moore and Hudson because it was below their detection limit which was 0.1-0.2%. Loeffler et. al [85] extended this study by producing H<sub>2</sub>O<sub>2</sub> up to 120K with Ar<sup>+</sup> and H<sup>+</sup> protons from 50-100 keV. These experiments explain the presence of H<sub>2</sub>O<sub>2</sub> on Europa is a consequence of radiolysis and photolysis of the water ice surface. They also showed that the production of hydrogen peroxide decreases with increasing temperature, but only at certain ion energies. This could explain the low concentration of H<sub>2</sub>O<sub>2</sub> found on Europa due to its high surface temperature. However, irradiation of ice films with 30 keV Ar<sup>+</sup>, Gomis et al. observed no temperature dependence. The discovery of H<sub>2</sub>O<sub>2</sub> and the likely presence of a subsurface ocean on Europa led to the idea of a radiation-driven ecosystem [23].

### 1.2.3 O<sub>2</sub> & O<sub>3</sub>

There are extensive laboratory data on radiation chemistry of ice; however, the kinetics of irradiation induced non-thermal production of oxygen is inconclusive. The oxygen visible reflectance measurement showed two absorptions at 577 nm and 627.5 nm on Ganymede [13], this closely resembles the reflectance spectra of solid-state oxygen [26, 134]. This led to the belief that it might be trapped within the ice (possibly in microbubbles with the presence of O<sub>3</sub> [60]) because the surface temperature is well above O<sub>2</sub> sublimation point, both on Ganymede and Europa. By now it is well known that irradiation is responsible for O<sub>2</sub> and there may be many different intermediates involve and complicated by the presence of surface impurities. However, we start at the very basic level by looking at pure water

ice as it is the main constituent on many of these icy surfaces. Many models have been proposed by radiation chemists; however, these proposed intermediates have never been identified experimentally by spectroscopic techniques.

Petrik et. al [111] proposed a multi-step model which involve a hydroperoxy ( $\text{HO}_2$ ) intermediate where the principle dissociation steps of water (Eq. 1.1 and 1.2) releases  $\text{HO}_2$  which follow by



Another model [140] with the same OH formation steps and intermediate as Petrik recognized instead that  $\text{O}_2$  is form by



Johnson et al. [65] proposed a model which involves an oxygen atom intermediate and was recently shown using the detection of isotopologues of ozone that O atom production occur in irradiated  $\text{H}_2\text{O}$  and  $^{18}\text{O}_2$  thin-film samples [30]. Using isotopic substituted  $^{18}\text{O}_2$ , Cooper et al. showed that the  $\text{O}_3$  produced by 0.8 MeV proton irradiation composed of both  $^{16}\text{O}$  and  $^{18}\text{O}$  and that more  $^{16}\text{O}$  are favored upon increasing irradiation dose. In summary, they suggest the O atom produced by  $\text{H}_2\text{O}$  excitation reacts with  $\text{O}_2$  to produce ozone, according to the Johnson model.

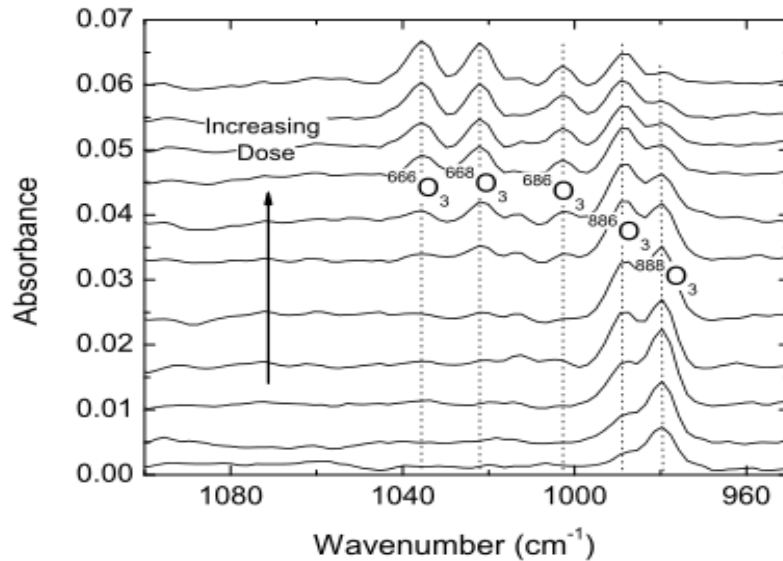


Figure 1.2: IR absorbance spectra of  $O_3$  isotopologues with increasing radiation dose [30].

While the isotopologues study of ozone strengthens the model by the Johnson model, it does not prove that this model is valid nor discredits the others. While these proposed models for the non-thermal production of  $O_2$  in ice via radiolytic processes [65, 140] are impressive in their own ways, sadly, none has been generally accepted. Furthermore, experimental observations and trapping of chemical intermediates is a difficult task given the elusive reactive nature of OH,  $HO_2$  and O atoms. In addition, the quantitation of  $O_2$  supposedly trapped in the ice surface has yet been determined. Since all of current models are based on irradiation of thin ice films, the new method propose in this research should be given consideration.

Ozone ( $O_3$ ) has also been tentatively detected on the trailing hemisphere of Ganymede [101] and exists stably in micro-bubbles as mixtures of  $O_2/O_3$  in the surface [60]. This observation also faces similar problem to  $H_2O_2$  because  $O_3$  has only been observed on Ganymede and the two satellites of Saturn; Rhea and Dione [102] and base on our current understanding from laboratory data that any ice surface under constant plasma bombardment will produce  $O_2$  and  $O_3$  [28]. Detection of  $O_3$  is an indirect measurement of  $O_2$ .

### 1.3 The Outer Solar System

The largest planet in our solar system: Jupiter has 63 moons but only four of which has been widely studied. These moons in order of orbital distance are Io, Europa, Ganymede, and Callisto. The flyby missions of Pioneer and Voyager in the 1970s gave us a wealth of information about the radiation environment of Jupiter. Jupiter's intrinsic magnetic field produces a magnetosphere so great that it extends a few hundred planetary radii away from Jupiter and is the largest object inside the heliosphere. This not only protects Jupiter from the solar wind, but also provides a radiation environment rich in energetic particles and is the source that drives surface chemistry on the satellites. The Galilean system is about 1 au beyond the frost line, so most molecules such as water ( $\text{H}_2\text{O}$ ), ammonia ( $\text{NH}_3$ ), and sulfur dioxide ( $\text{SO}_2$ ) are present in solid form and the reason why the surface of Europa is covered in water ice presumably kilometers thick. Radiation processing of the ice surface is ubiquitous to these regions but is not limited to the outer solar system bodies. These satellites also receives about twenty five times less sunlight than Earth, therefore, surface and atmospheric chemistry is dominated by radiolysis. Io is the main source for particles and a great contributor to the plasma density of Jupiter's magnetosphere. The composition of this plasma contains mostly  $\text{S}^{n+}$  and  $\text{O}^{n+}$  ions [9] due to a predominately  $\text{SO}_2$  ice surface. These particles most likely would end up impacting the surface of neighboring satellites fueled by the acceleration from the magnetic field lines.

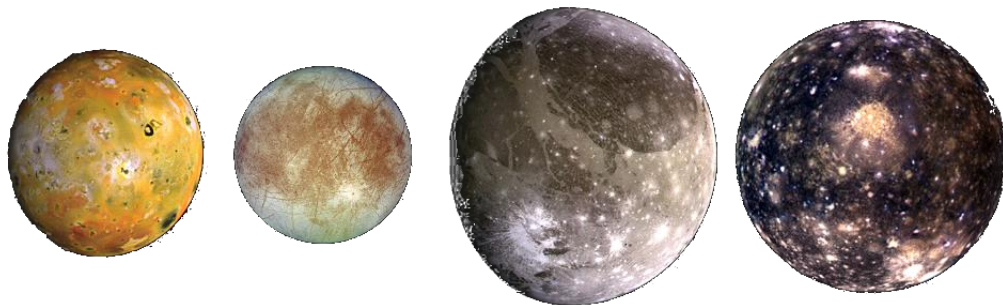


Figure 1.3: Galilean satellites. From left to right: Io, Europa, Ganymede, and Callisto. [NASA Photojournal]

Table 1.1: Physical parameters of the Galilean satellites [NASA Fact Sheet].

	Radius (km)	Density (kg/m <sup>3</sup> )	Escape velocity (km/s)	Atmosphere (Major)
Io	1821	3.53	2.6	SO <sub>2</sub>
Europa	1560	3.01	2.0	O <sub>2</sub>
Ganymede	2631	1.94	2.7	O <sub>2</sub>
Callisto	2410	1.83	2.4	CO <sub>2</sub>
Earth	6378	5.51	11.2	N <sub>2</sub> , O <sub>2</sub>

## Europa

With a diameter of about 3121 km, Europa is the smallest of the four Galilean moons (Figure 1.4). The surface is composed of predominately amorphous water ice which makes up the light regions of the surface. Dark terrains also appear on the surface that is thought to be from hydrated materials. These materials resemble that of magnesium hydrates, sodium hydrates, and sulfate hydrates [34]. A mixture of all these hydrates material could be present on the surface due to similarities in their spectra. Europa might contain a subsurface liquid ocean and subduction could be a mechanism for resurfacing of materials to and from the surface. The SO<sub>2</sub> present on Europa’s surface may be exogenic. Sulfur rich materials ejected from volcanoes on Io possibly transported to Europa via the magnetic field lines. Also, the presence of carbon dioxide (CO<sub>2</sub>) coupled with radiolysis may play an important role in the darkening of the terrains on the trailing side of Europa [48].

Although tenuous, Europa has an oxygen atmosphere [46] that may come from charged-particle sputtering of the surface ice [79]. Based upon laboratory evidence, a proton [140] or electron [65, 110, 156] irradiated water ice surface will produce O<sub>2</sub> molecules. The process of erosion may be due to sputtering of the ice surface [11]. Oxygen molecules are insoluble in water ice since it has a low binding energy to the surface. Therefore, any oxygen formed will most likely leave the surface unless it is trapped in pores or defects [60]. Most would end up escaping into space given the low gravitational energy of Europa. Since Europa

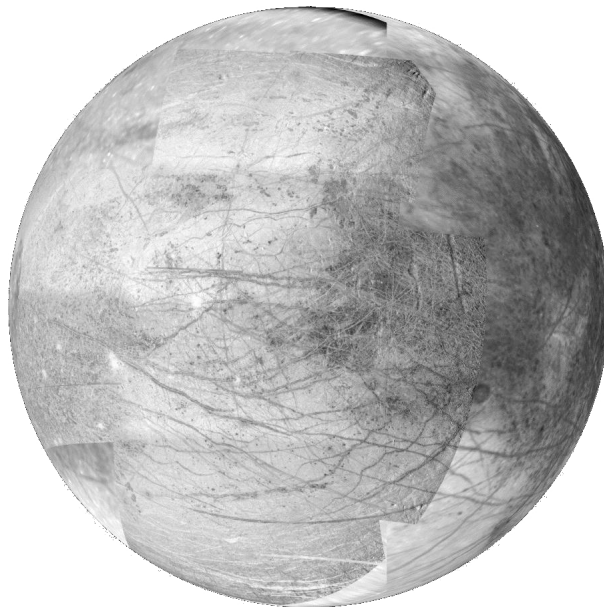


Figure 1.4: Image of Europa taken by the Galileo orbiter. [NASA Photojournal]

is geologically active, the oxygen source could be from cryovolcanism like on Enceladus, however, cryovolcanic activity at Europa has to be detected. Another possibility is that oxygen may have come from Io. Sulfur dioxide ( $\text{SO}_2$ ) ejected from volcanoes on Io and subsequently dissociated into  $\text{S}^+$ ,  $\text{O}^+$  and  $\text{O}_2^+$  could help form most of Europa's oxygen micro-atmosphere.

The main highlight of Europa is the present of a subsurface liquid ocean that is sustained by tidal heating [118] which may harvest life in hydrothermal vents on the ocean's floor like on Earth [145]. A liquid ocean is possible as evidence of a sodium atmosphere points to the sputtering of resurfaced salty materials [10, 59, 66, 82].

## **Io**

Important measurements of the ionospheres and the local plasma density have been made by the instruments aboard the Galileo spacecraft that gave us a good understanding about physical environments of this satellite (Figure 1.5). The closet flyby approach of Io was made on Feb. 22, 2000 at an altitude of 197.9 km by the Galileo spacecraft. This innermost moon

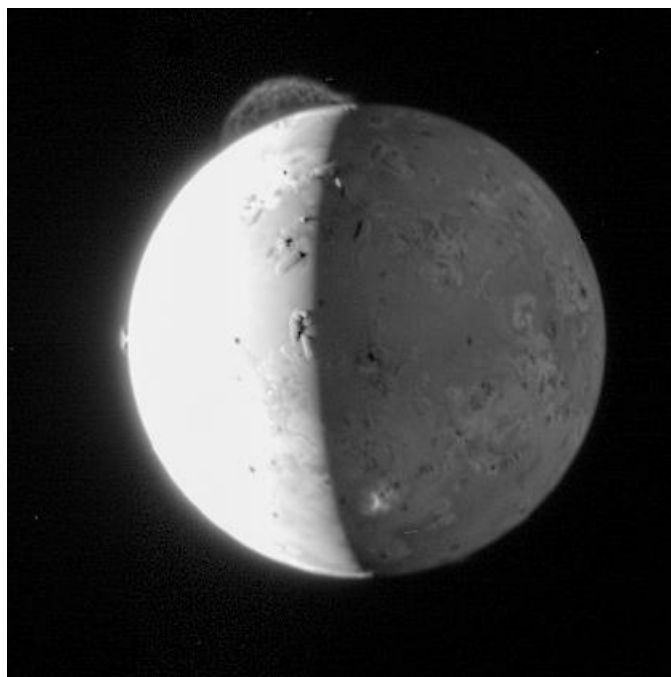


Figure 1.5: Volcanic plume on Io. Imaged by New Horizons. [NASA Photojournal]

of Jupiter is the only known body other than Earth to have active volcanic activities. The energy required for this stems from tidal forces and resonating orbits with the neighboring moons. Volcanic ejections of particles produce high velocity plumes that extend hundreds of kilometers into the atmosphere [39]. In contrast to the other three Galilean satellites, the surface and atmosphere of Io is mostly  $\text{SO}_2$  [32, 38, 97, 100] with little or no evidence of  $\text{H}_2\text{O}$ . Water was likely lost over time due to sputtering by charged-particles [114]. Io is believed to be a major source of sulfur and oxygen in the Galilean system which contributes to the radiation flux density to the other three Galilean moons. Volcanism on Io provides a means for resurfacing of sulfur compounds. Molecules ejected by the volcanic plumes on Io, containing mainly sulfurs and oxygens, are carried to the other Galilean satellites by the magnetic field.

Io is one of the main examples of the resurfacing model where molecules are ejected and fall back down to the surface. Although highly oxidizing, due to the lack of water on its surface, Io does not experience the same radiolytic chemical processes as on Europa,

Ganymede or Callisto. Laboratory experiments have shown that the irradiation of SO<sub>2</sub> ices produced only sulfur trioxide (SO<sub>3</sub>), sulfuric acid (H<sub>2</sub>SO<sub>4</sub>), and the sulfur allotrope (S<sub>8</sub>) [96]. It is expected that SO<sub>3</sub> is present on Io, however, it has not been detected possibly due to low concentrations (<1%) and is below the detection limit of our instruments [98].

### **Ganymede and Callisto**

Ganymede was discovered in 1610 by Galileo Galilei and is the largest known satellite in our solar system. Molecular oxygen was first identified on its surface in 1995 [135]. Visible reflectance spectra shows oxygen to be present on the surface [13] that closely resembles the laboratory measured reflectance spectra of  $\gamma$ -oxygen [26, 134]. The oxygen absorptions arised from the forbidden electronic transition from the ground state ( $X^3\Sigma_g^-$ ) to the first excited state ( $a^1\Delta_g$ ) of O<sub>2</sub> [5, 72]. UV and energetic particle bombardments could be responsible for the O<sub>2</sub> production which also produces micropores to trap them [60]. However, it is unclear how oxygen can be trapped in the ice surface since Ganymede's average surface temperature range is 90-152K [105], this is much higher than the sublimation temperature of oxygen in vacuum (30K). No one has yet to come up with an ideal model to explain this phenomenon. In addition to molecular oxygen and ozone in the surface ice, atomic hydrogen has been detected in the exosphere and thought to have come from the dissociation of water vapor similar to processes occuring in the Earth's atmosphere [6].

Callisto is the outermost satellite of the four major Galilean moons. Its' surface is heavily cratered by primordial impacts and is the oldest surface in the solar system due to little to no geologic and resurfacing activities. The lack of surface chemistry on the surface put Callisto at the bottom of the list in terms of relevance compare to other satellites. Like Europa and Ganymede, condensed molecular oxygen was also identified on Callisto [134]. An SO<sub>2</sub> absorption was also identified similar to the band on Europa's trailing hemisphere at 280nm [102]. Being a mostly water ice surface, Callisto could have received it's SO<sub>2</sub> by resurfacing from Io. All four Galilean satellites contains tenous atmosphere characteristic of its' surface. Callisto atmosphere consist of mostly carbon dioxide (CO<sub>2</sub>) molecules [15].

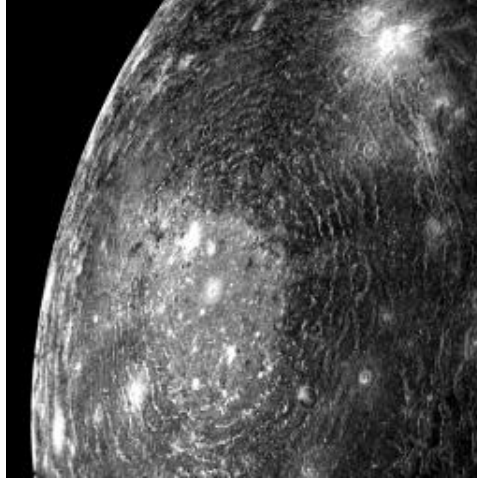


Figure 1.6: Image of a cratered Callisto. [NASA Photojournal]

### **Saturnian system**

Saturn has the second largest magnetic field in the solar system but unlike Jupiter, Saturn's magnetosphere has an abundance of water neutrals of OH, O, H, H<sub>2</sub>O, and H<sub>2</sub>. A giant toroidal cloud containing OH radicals that stretches from the inner edge of Saturn's main ring to Enceladus (E) was discovered in 1993 [124]. This finding was important since OH radicals were detected in irradiated water ice and an important component of resurfacing chemistry. The formation of OH radicals occurs when H<sub>2</sub>O molecules are dissociated by the local energetic plasmas. This OH presence was predicted to have an H<sub>2</sub>O source that originates from Enceladus [69].

The magnetosphere of Saturn also contains molecular oxygen which comes from radiation-induced decomposition of ice from its moons. It was not surprising when the Cassini spacecraft detected O<sub>2</sub><sup>+</sup> and O<sup>+</sup> ions about the rings of Saturn [141, 151] forming an oxygen atmosphere. A major source of this ionosphere was first thought to be through UV photolysis of the ring's icy grains [61] due to low plasma densities surrounding the main rings. However, this source is now considered too small to account for the entire O<sub>2</sub> present. There must be another source of oxygen at the rings. One possibility is that Saturn's moon Enceladus [16] and its toroidal cloud of neutrals is responsible for the oxygen atmosphere. Deposition of water products from Enceladus plumes onto the ring components is a possible

process that occurred over time and could be a model for resurfacing chemistry. Saturn's ring components are made up of dirty ices ranging from micrometers to boulder in sizes. The ring's environment is composed of charged particles, electrons, and UV photons. The oxygen atmosphere present there is similar to the one on Europa where the source was predicted to be from sputtering or decomposition of the ice via energetic ions and electrons [67]. Given the similarity that both of these bodies have a water ice surface, it is likely they share a common process in atmospheric productions of  $O_2$ .

## Chapter 2: Experimental

### Traditional Experiments

Traditional laboratory radiation experiments (Figure 2.1) were performed by irradiation of H<sub>2</sub>O ice films in which radicals (e.g. OH) are formed and reacted in-situ. Exposed to the ice are radiation sources such as electrons, photons, or energetic ions with varying energy and dosage. Chemical changes within the ice were then measured with infrared or ultraviolet spectroscopy. In desorption or sublimation studies, quadrupole mass spectrometers (QMS) are used. These techniques have been used extensively in the radiation studies of ice [54, 55, 95].

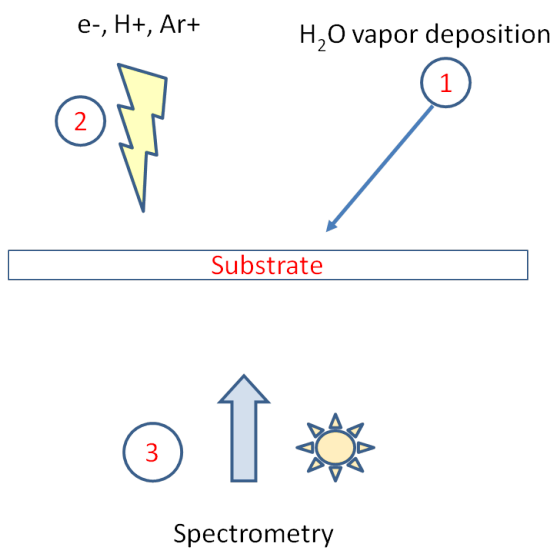


Figure 2.1: Schematic of typical traditional experiments.

The difference between this method of studying radicals and the matrix isolation technique is the exclusion of the inert gas. In matrix isolation, photolysis is often used for in-situ excitation as opposed to electrons or protons. This is a precaution against sputtering or sublimation of the matrix. Radiation sources typically used in traditional experiments are UV photons, electrons (eV), protons (keV), and heavy ions (Ne<sup>+</sup>, Ar<sup>+</sup> MeV). Table 2.1 summarizes the different types of radiations and temperatures used in the study of radiation chemistry of water ice over the years.

Table 2.1: Summary of radiation and temperatures in irradiated ice experiments.

Radiation	T (K)	Ice Thickness	Products	Ref.
0.8 MeV H <sup>+</sup>	16-80	3 $\mu\text{m}$	H <sub>2</sub> O <sub>2</sub>	[94]
30 keV H, C, N, O, Ar <sup>+</sup>	16, 77	0.5 $\mu\text{m}$	H <sub>2</sub> O <sub>2</sub>	[42]
100 keV e <sup>-</sup>	50-155	50-100 ML	D <sub>2</sub> , O <sub>2</sub>	[44]
50-100 keV Ar <sup>+</sup> , 100 keV H <sup>+</sup>	20-120	1-1.9 $\mu\text{m}$	H <sub>2</sub> O <sub>2</sub>	[85]
5 keV e <sup>-</sup>	12-90	115 nm	H <sub>2</sub> O <sub>2</sub> , O <sub>2</sub> , H <sub>2</sub>	[156]

There are two structures of water ice that are equally important to the study of surfaces in space. In the laboratory, amorphous ice is formed by condensing water vapor onto a cold surface below 100K and warming this ice to 120K produces a crystalline ice sample [62]. Amorphous ice is typically made in irradiated experiments where deposition temperature is low. Small film thickness also results in an ice with small grain sizes and low porosities. The spectral properties are different between polycrystalline and amorphous ice. The former has a sharper water peak features in the far-IR region [54]. The most important step in these experiments is to make sure there is no trace gases in the water used as vapor for deposition. In this step, distilled water is repeatedly frozen with liquid nitrogen and defrosted in vacuum [120, 156], using the freeze-thaw-pump method to ensure trace gases are pumped out from the water sample.

The main experimental setup for a typical irradiation lab consists of a vacuum chamber, a turbo molecular pump, a helium cooled closed cycle refrigerator. Radiation sources come from Van de Graaf accelerators (protons) and electron guns. Microbalances are used in sputtering experiments or for determining sample thickness [122]. Analysing samples usually require the use of mass/FT-IR/UV spectrometers.

The use of a microbalance to determine thickness only requires the knowledge of the density. Another useful way of determining a sample thickness without the use of a microbalance is by knowing the A-value or the intrinsic strength of an IR band. These values can be found in the literature for most oxidants like H<sub>2</sub>O<sub>2</sub> [85], H<sub>2</sub>O [52], and O<sub>3</sub> [30]. The column density of a molecule is calculated by,

$$N = \frac{2.303 \int A(\nu) d\nu}{A} \quad (2.1)$$

where A is the band strength and  $\int A(\nu) d\nu$  is the band integration of a peak corresponding to the A value. The units for N is molecule/cm<sup>2</sup>. Sample thicknesses are found by simply dividing N by the density (molecule/cm<sup>3</sup>). Calculating the column density helps determine the yield of a specific product in an irradiated ice sample.

### **Redeposition Experiments**

This current approach is very similar to experiments done in the past except radicals are produced (OH/O-atoms) in the gas phase from a tesla coil discharge and deposit alongside water (Figure 2.2). Mixtures of water and a carrier rare gas (~1:100 ratio) are then deposited onto a cold substrate above the sublimation temperature of the rare gas (> 20K) which form an ice sample. While trace amounts of rare gas can be physically trapped in the ice, this is negligible as it is inert and does not interact with the water radicals. A 6" cylindrical vacuum chamber has a base pressure  $\sim 1 \times 10^{-8}$  Torr maintained by a Leybold turbo-molecular pump. Rare gases used were neon, helium, and argon. Argon was used for matrix isolation experiments while neon and helium were used for ice experiments.

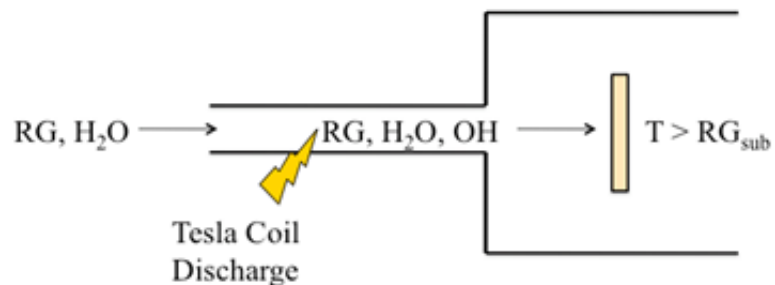


Figure 2.2: Deposition of radiowave discharged H<sub>2</sub>O/Rare Gas mixture.

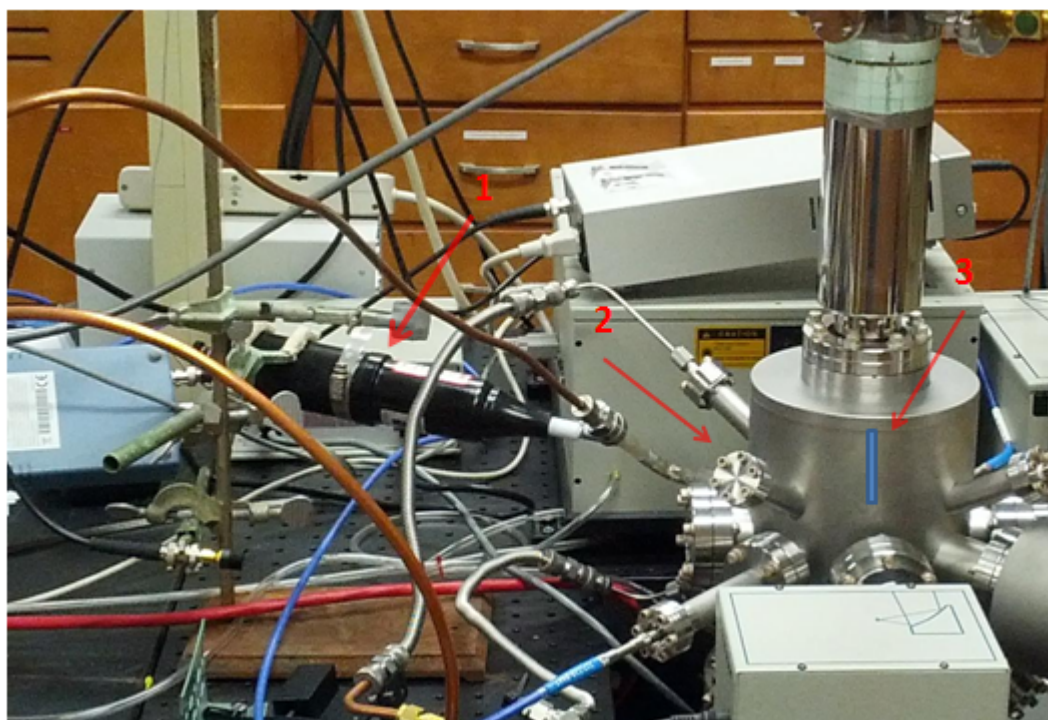


Figure 2.3: Actual deposition setup. 1. Tesla coil 2. Water mixtures flow through glass tube where discharge occurs 3. 360 degrees rotatable sample holder 90 degree facing inlet port.

The gas mixtures are mixed in a vacuum stainless steel manifold with liter size glass bulb reservoirs (Figure 2.4). The gases are flown through a 3/8" glass tube attached to the vacuum chamber. The distance from the glass tube to the sample holder is about 1/2". Attached to the glass tube is a tesla coil where an electrical discharge subjects the water to

dissociations and radical formation prior to deposition onto the substrate. The resulting ice is a mixture of H<sub>2</sub>O/OH or O-atom rich ice that yield oxidants. The inclusion of the RG is important to sustain the discharge and prevent significant gas-phase reactions between reactive species. Samples were deposited on a highly polished KBr or BaF<sub>2</sub> substrate.



Figure 2.4: Stainless steel gas manifold and two 1L glass bulbs used for mixing and storing water and rare gas mixtures.

The instruments used for this experiment are: Newport MIR8025 FTIR spectrometer, Extorr (XT100M) quadruple mass spectrometer (QMS), and a DH-2000 Ocean Optics UV-vis spectrometer. The FTIR spectrometer is used for measuring spectra at 4 cm<sup>-1</sup> resolution in transmission mode for both matrix isolated and ice experiments. The quadruple mass spectrometer is used for qualitative temperature program desorption experiments. The UV-vis spectrometer is used for measuring radicals in matrix isolation experiments with argon or to detect infrared inactive species like O<sub>2</sub>. The stainless steel vacuum chamber is attached to a cold finger and a turbo molecular pump where the base pressure is 10<sup>-8</sup> torr. The sample window is connected to the cold finger and enclosed in a radiation shield which

can be cooled down to 6K. The cold finger can rotate 360° to deposit samples and then to other ports for measurement of the sample. A diagram of the relative placement of the instruments connected to the vacuum chamber is on Figure 2.5.

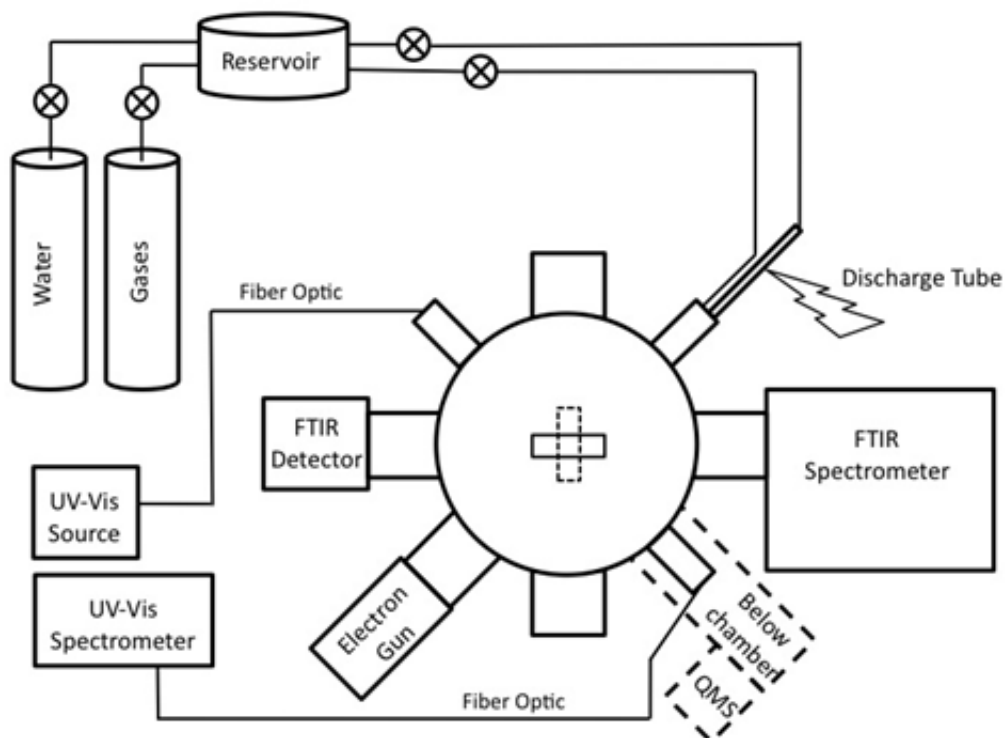


Figure 2.5: Diagram of stainless steel vacuum system.

## Chapter 3: Results

### 3.1 Data

This project started out as matrix isolation experiments on the OH-H<sub>2</sub>O complex in neon matrices as an extension to the previous work by Cooper et al. [27] in argon. As with all matrix isolation of neon, deposition temperature should be below 10K, however, a sample was accidentally deposited at 20K and a new spectrum was obtained that resembled those of irradiated ice experiments. It was apparent that the rare gas did not deposit, thus creating an ice sample. It was determined that reactions in the solid-phase between radicals, produced in the discharge, had occurred to form oxidants. This is deduced from the absence of H<sub>2</sub>O<sub>2</sub>, O<sub>3</sub> and O<sub>2</sub> (forbidden IR) in matrix isolated samples. Matrix isolation techniques were then used for trapping and quantifying radicals. This provides important insight into the role of reactive species in water ice. OH, O, and HO<sub>2</sub> can all be trapped in argon matrices, however, only OH can be quantified due to the current lack of data on the intrinsic band strengths for the other radicals. The sublimation of neon rare gas in vacuum was observed by depositing water and neon mixtures at 6K, at this temperature, neon should form matrices with water. As the sample is warmed to 20K, the sublimation of neon can be seen from the resulting infrared spectrum (Figure 3.1). The broad water peak at 3300 cm<sup>-1</sup> is a signature of the pure ice spectrum.

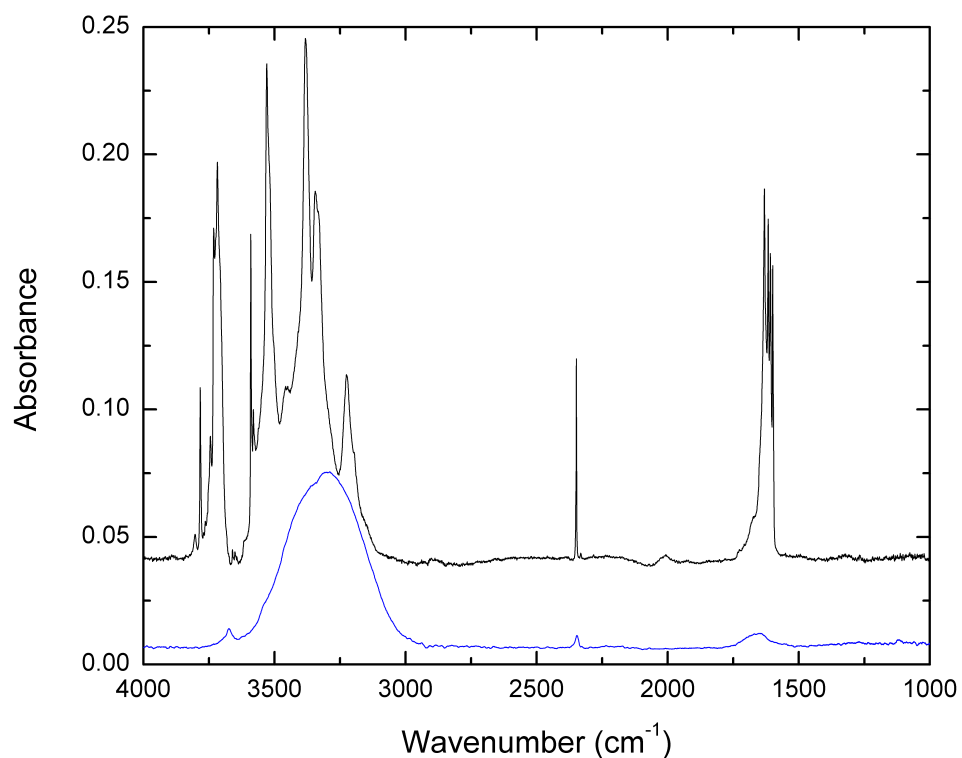


Figure 3.1: IR spectrum of matrix isolated H<sub>2</sub>O:Ne (1:100) at 6K (top) and after warming to 20K (bottom).

At 20K, neon is sublimed from the sample leaving a water rich sample. Alternatively, sublimations can be estimated by mass spectrometry where H<sub>2</sub>O:RG samples are warmed with the mass spectrometer running. This method was used to determine the sublimation temperature of rare gas in the vacuum chamber. It was determine that argon sublimes at above 40K. Helium was also used for the ice experiments, but this rare gas does not condense in vacuum.

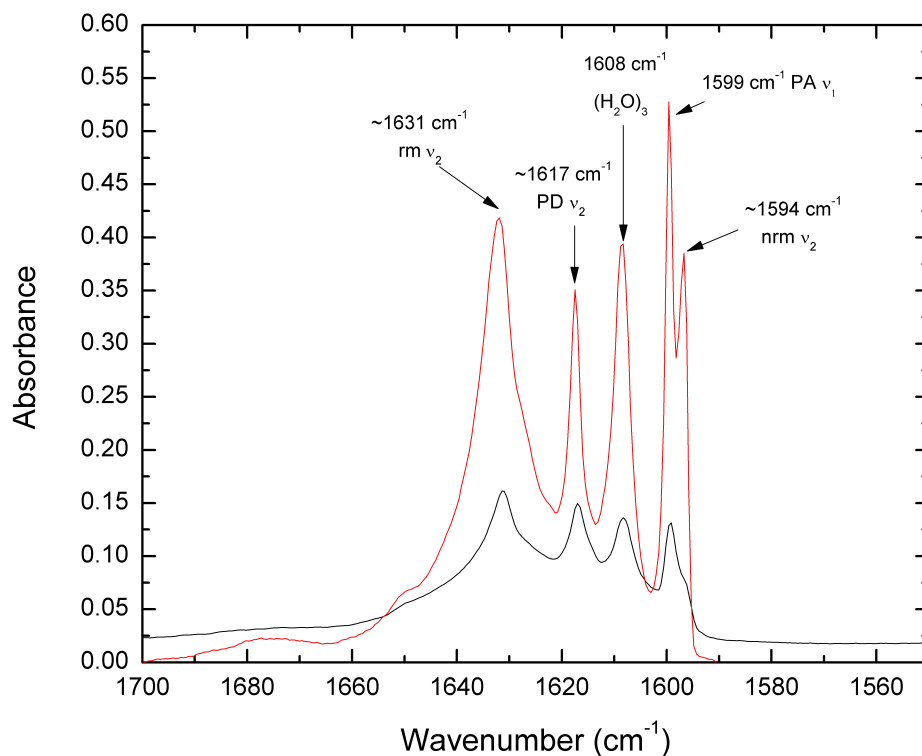


Figure 3.2: 1750 to 1550  $\text{cm}^{-1}$  matrix isolated  $\text{H}_2\text{O}:\text{Ne}$  at 6K without discharge (bottom) and with discharge (top). PA = proton acceptor, PD = proton donor.

Figure 3.2 and 3.3 shows that matrix isolated experiments with and without discharge are very similar. This is due to the dilution of water and the quenching of radical species by the rare gas and the immobility of OH radicals due to the low temperature. The assignments of these water bands matched several previous literature sources [8, 18, 19, 20]. Our initial examination of OH- $\text{H}_2\text{O}$  complexes in neon were unsuccessful. The presence of significant  $\text{H}_2\text{O}$  multimers revealed our Ne matrix was “soft”. This allows the diffusion of species, resulting in the formation of the multimers, and so the matrix sample did not accurately represent the gas-phase composition. Table 3.1 summarizes the band assignments of  $\text{H}_2\text{O}$  monomers and multimers in the neon matrix samples.

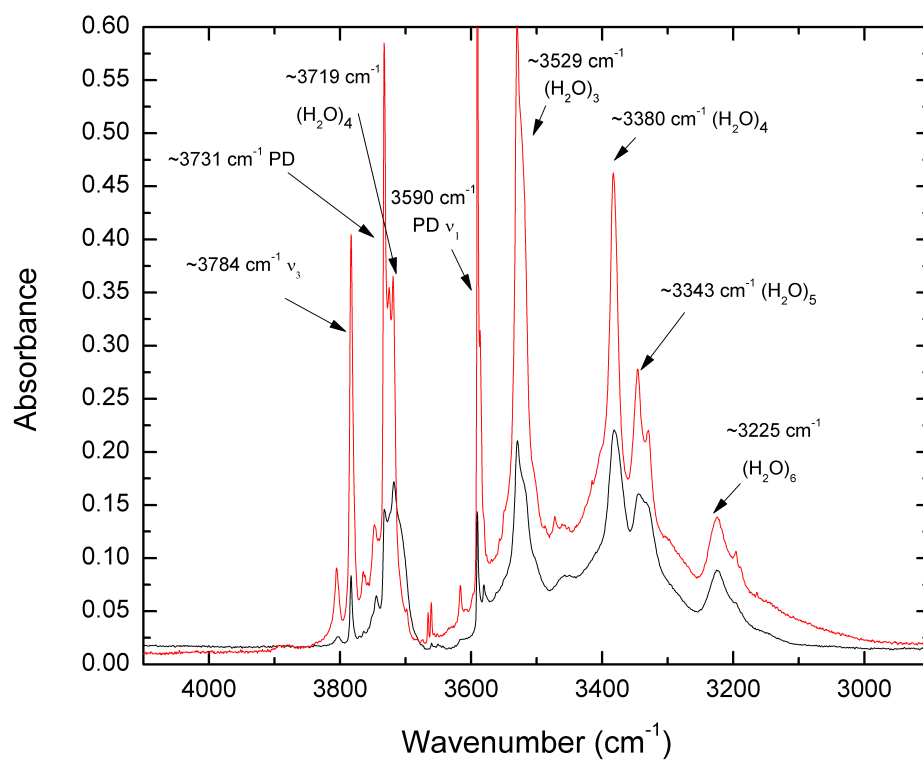


Figure 3.3: 4100 to 2900 cm<sup>-1</sup> matrix isolated H<sub>2</sub>O:Ne at 6K without discharge (bottom) and with discharge (top).

Table 3.1: Band assignments ( $\text{cm}^{-1}$ ) of  $(\text{H}_2\text{O})_n$  in matrix isolated  $\text{H}_2\text{O}:\text{Ne}$  (1:100) compare to literature. nrm = non-rotating monomer.

	This work	Literature	References
<hr/> $\text{H}_2\text{O}$ monomer <hr/>			
$\nu_2$ nrm	1596.7	1594.75 <sup>a</sup> , 1595.8 <sup>b</sup>	<sup>a</sup> Ref. [8], <sup>b</sup> Ref. [50]
$\nu_2$ rm	1632.0	1630.8 <sup>b</sup>	
<hr/> $(\text{H}_2\text{O})_2$ <hr/>			
$\nu_2$ PA	1599.7	1599.2 <sup>ac</sup>	<sup>c</sup> Ref. [19]
$\nu_2$ PD	1617.5	1616.5 <sup>a</sup> , 1616.4 <sup>c</sup>	
$2\nu_2$ PA	3163.9	3163 <sup>a</sup>	
$2\nu_2$ PD	3195.9	3193.7 <sup>a</sup>	
$\nu_1$ PD	3590.4	3590.4 <sup>c</sup> , 3590.5 <sup>a</sup> , 3590 <sup>b</sup>	
$\nu_1$ PA	3660.9	3660.5 <sup>a</sup> , 3660.6 <sup>c</sup>	
$\nu_1$ PA	3673.7	3674 <sup>c</sup>	
$\nu_3$ PD	3732.7	3733.7 <sup>ac</sup>	
<hr/> $(\text{H}_2\text{O})_3$ <hr/>			
	1608.6	1608.3 <sup>d</sup> , 1608.2 <sup>e</sup>	<sup>d</sup> Ref. [142], <sup>e</sup> Ref. [18]
	3189.3	3189.3 <sup>d</sup>	
weak shoulder		3517.5 <sup>d</sup> , 3518 <sup>be</sup>	
	3472.2	3472.2 <sup>d</sup>	
	3529.7	3529.5 <sup>d</sup> , 3529.6 <sup>e</sup> , 3529 <sup>b</sup>	
	3725	3725.5 <sup>d</sup> , 3725 <sup>e</sup>	
<hr/> $(\text{H}_2\text{O})_4$ <hr/>			
	3383	3383 <sup>bf</sup>	<sup>f</sup> Ref. [20]
	3719	3718.5 <sup>f</sup>	
<hr/> $(\text{H}_2\text{O})_5$ <hr/>			
	3345.9	3345 <sup>bf</sup>	
<hr/> $(\text{H}_2\text{O})_6$ <hr/>			
	3224.5	3224 <sup>bf</sup>	
<hr/> cyclic- $(\text{H}_2\text{O})_6$ <hr/>			
	3329.5	3330 <sup>f</sup> , 3329 <sup>b</sup>	

In order to determine the composition of the discharge, matrix isolated experiments in argon were done. Matrix isolation of water in argon has been well studied, OH has been observed in argon at  $3550\text{ cm}^{-1}$  [27].  $\text{HO}_2$  has been observed at  $3413\text{ cm}^{-1}$ ,  $1389\text{ cm}^{-1}$ , and  $1100\text{ cm}^{-1}$  [28]. Triplet oxygen atoms, observed as the  $\text{H}_2\text{O}\cdot\text{O}$  complex is seen at  $3730\text{ cm}^{-1}$  [107].  $\text{H}_2\text{O}\cdot\text{HO}$  complexes absorb in the infrared at  $3452\text{ cm}^{-1}$ ,  $3442\text{ cm}^{-1}$ , and  $3428\text{ cm}^{-1}$  [27]. So, matrix isolation experiments show the presence of OH,  $\text{HO}_2$  (Figure 3.4) and O atoms (Figure 3.5), as the direct result of the discharge.

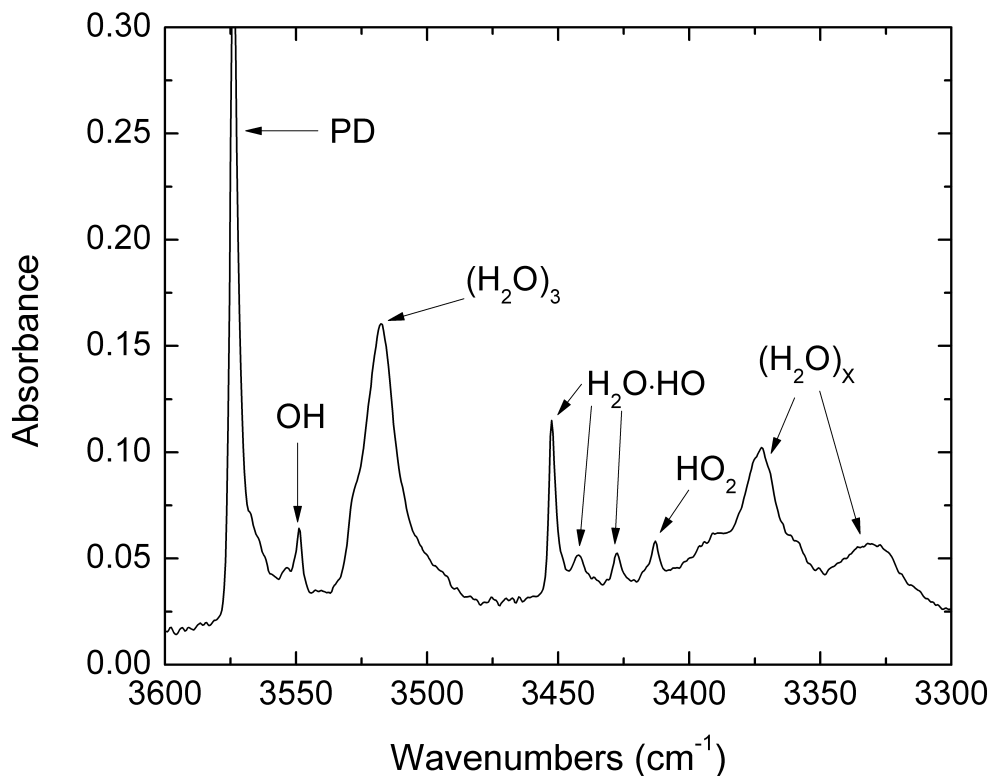


Figure 3.4: OH and  $\text{HO}_2$  in  $\text{H}_2\text{O}:\text{Ar}$  1:100 matrix.

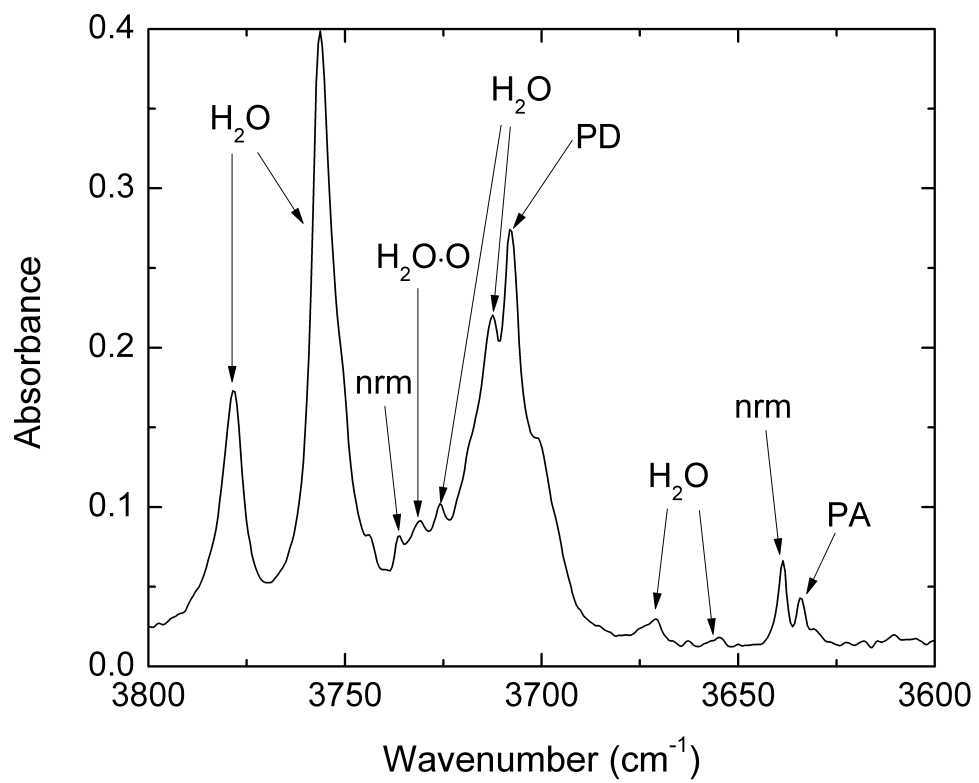


Figure 3.5: Triplet O atom in H<sub>2</sub>O:Ar 1:100 matrix.

The initial amount of OH radicals was found by depositing discharged water and argon at 6K. The matrix isolated UV spectrum (Figure 3.6) shows OH at  $\sim 312$  nm. Using the A-value of OH ( $1.16 \times 10^{-15}$  cm molecule $^{-1}$ ) [139], a column density of OH is estimated to be  $6.39 \times 10^{16}$  molecules cm $^{-2}$ . This is approximately 1.5% by number relative to H<sub>2</sub>O. This amount is presumably the initial OH concentration deposited in the ice experiments to form oxidants.

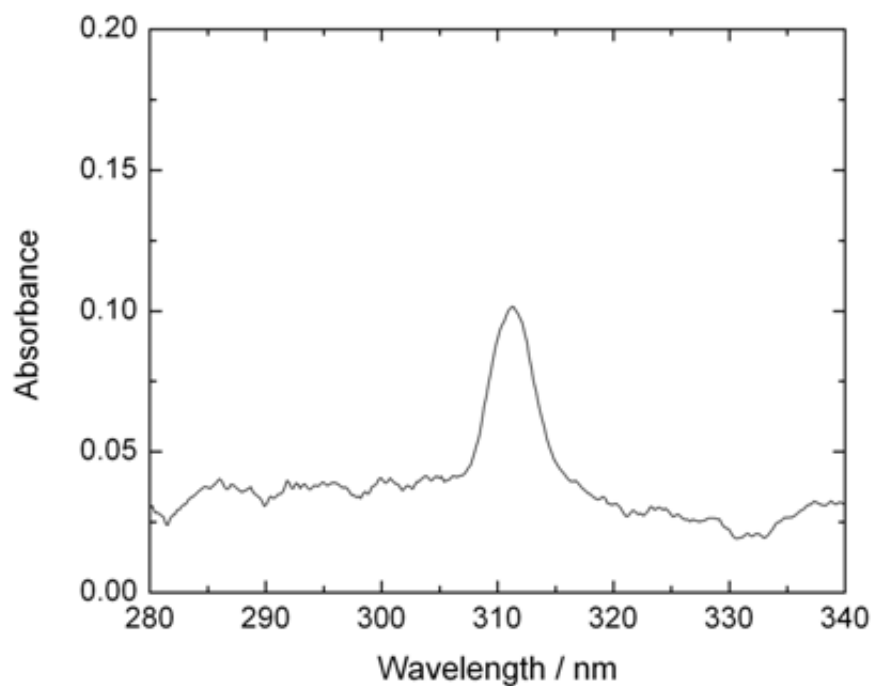


Figure 3.6: OH absorption in the UV.

Figure 3.7 and 3.8 shows the spectra of deposition for H<sub>2</sub>O:He and H<sub>2</sub>O:Ne respectively. It is apparent that hydrogen peroxide formation is favored at the lower temperatures for both rare gas depositions. For helium, however, H<sub>2</sub>O<sub>2</sub> absorptions at the 2850 cm<sup>-1</sup> bands are visible up to 80K compare to neon where it became undetectable past 60K.

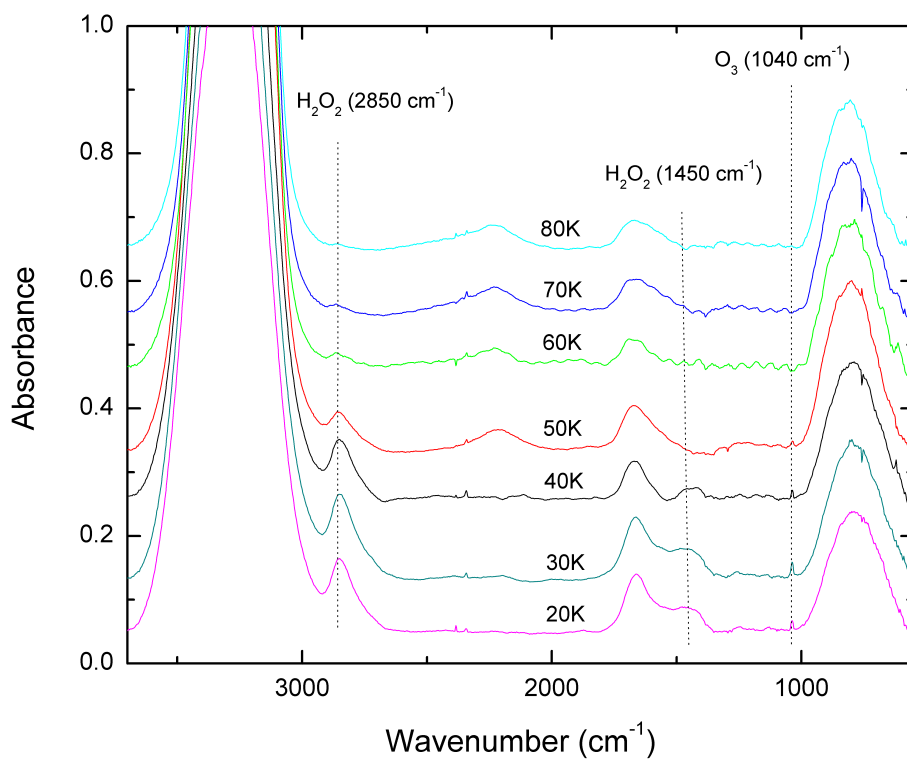


Figure 3.7: Helium and H<sub>2</sub>O mixtures 1:100 ratios deposited from 20K to 80K in 10K interval.

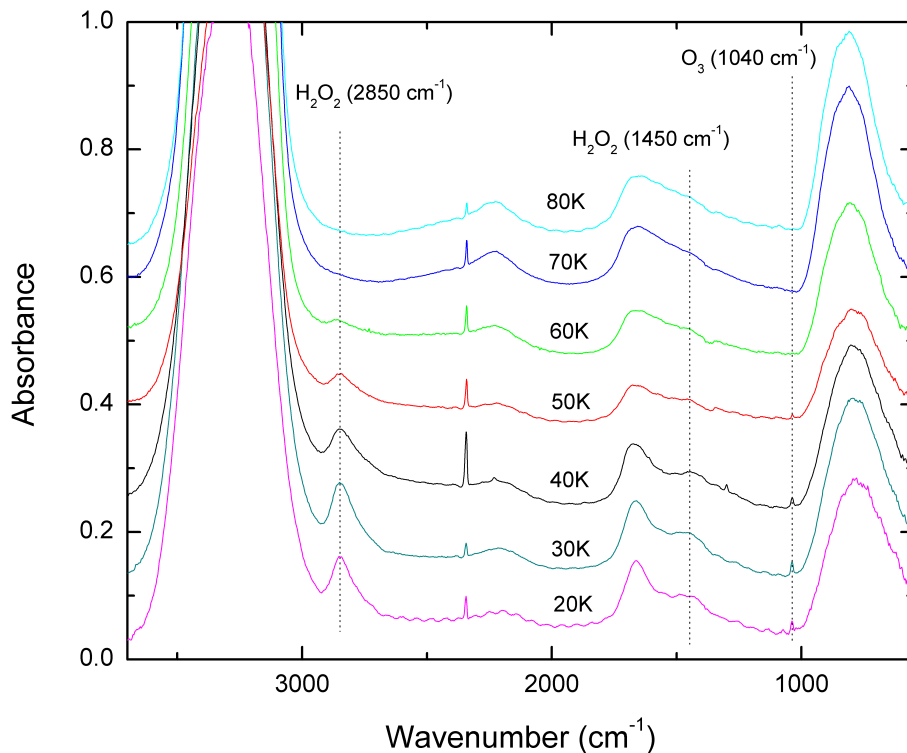


Figure 3.8: Neon and H<sub>2</sub>O mixtures 1:100 ratios deposited from 20K to 80K in 10K interval.

From Equation 2.1 and using A-values of  $5.7 \times 10^{-17}$  cm molecule<sup>-1</sup>,  $2.8 \times 10^{-17}$  cm molecule<sup>-1</sup>, and  $1.4 \times 10^{-17}$  cm molecule<sup>-1</sup> for H<sub>2</sub>O<sub>2</sub> (2850 cm<sup>-1</sup>) [85], H<sub>2</sub>O (760 cm<sup>-1</sup>) [52] and O<sub>3</sub> (1040 cm<sup>-1</sup>) [30] respectively, the relative column densities and sample thickness were determined (Table 3.2). The sample thickness ranges from 0.5 to 1  $\mu$ m. There seem to be no correlations between the ice thickness and H<sub>2</sub>O<sub>2</sub> concentration. H<sub>2</sub>O<sub>2</sub> and O<sub>3</sub> production is only affected by deposition temperature. O<sub>3</sub> is also favored at low temperature. OH radicals are known to be mobile in water ice above 80K so it was remarkable to see variations in compositions below the temperature range of OH mobility. OH radicals are also known for the destruction of H<sub>2</sub>O<sub>2</sub>, so perhaps at higher temperatures the destruction processes are greater than formation. These measurements raise important questions about

the formation and destruction of  $\text{H}_2\text{O}_2$  and  $\text{O}_2$  which is the main source for  $\text{O}_3$ . Up to 8.6% of  $\text{H}_2\text{O}_2$  relative to water was produced by the discharge deposition of an equivalent of  $\sim 3$  torr of water. In proton irradiated experiments,  $\text{H}_2\text{O}_2$  production is also favored at lower temperature, however, the yield is around 0.1-1% [85, 94], compared to heavy ion irradiation at around 6% [42].

Table 3.2: Column densities and thickness of  $\text{H}_2\text{O}:\text{He}$  and  $\text{H}_2\text{O}:\text{Ne}$  1:100 ice. \*Concentration below detection limit of instrument.

$\text{H}_2\text{O}:\text{He}$					
T(K)	Density $\text{H}_2\text{O}$ (molecule- $\text{cm}^{-2}$ )	Density $\text{H}_2\text{O}_2$ (molecule- $\text{cm}^{-2}$ )	Density $\text{O}_3$ (molecule- $\text{cm}^{-2}$ )	$\text{H}_2\text{O}_2/\text{H}_2\text{O}$ (%)	Thickness ( $\mu\text{m}$ )
20	$1.6 \times 10^{18}$	$1.2 \times 10^{17}$	$1.0 \times 10^{16}$	7.7	0.7
30	$1.7 \times 10^{18}$	$1.4 \times 10^{17}$	$1.5 \times 10^{16}$	8.6	0.7
40	$1.8 \times 10^{18}$	$1.1 \times 10^{17}$	$8.3 \times 10^{15}$	6.0	0.8
50	$2.0 \times 10^{18}$	$4.6 \times 10^{16}$	$4.2 \times 10^{15}$	2.3	0.9
60	$1.9 \times 10^{18}$	$1.1 \times 10^{16}$	*	0.6	0.8
70	$1.9 \times 10^{18}$	$6.4 \times 10^{15}$	*	0.3	0.8
80	$1.7 \times 10^{18}$	$1.9 \times 10^{15}$	*	0.1	0.7
$\text{H}_2\text{O}:\text{Ne}$					
20	$1.7 \times 10^{18}$	$1.1 \times 10^{17}$	$1.2 \times 10^{16}$	6.7	0.7
30	$1.9 \times 10^{18}$	$1.4 \times 10^{17}$	$1.3 \times 10^{16}$	7.1	0.8
40	$1.7 \times 10^{18}$	$9.1 \times 10^{16}$	$7.9 \times 10^{15}$	5.2	0.7
50	$1.2 \times 10^{18}$	$3.7 \times 10^{16}$	$2.4 \times 10^{15}$	3.2	0.5
60	$1.7 \times 10^{18}$	$1.3 \times 10^{16}$	*	0.8	0.7
70	$2.4 \times 10^{18}$	*	*	–	1.0
80	$2.3 \times 10^{18}$	*	*	–	0.9

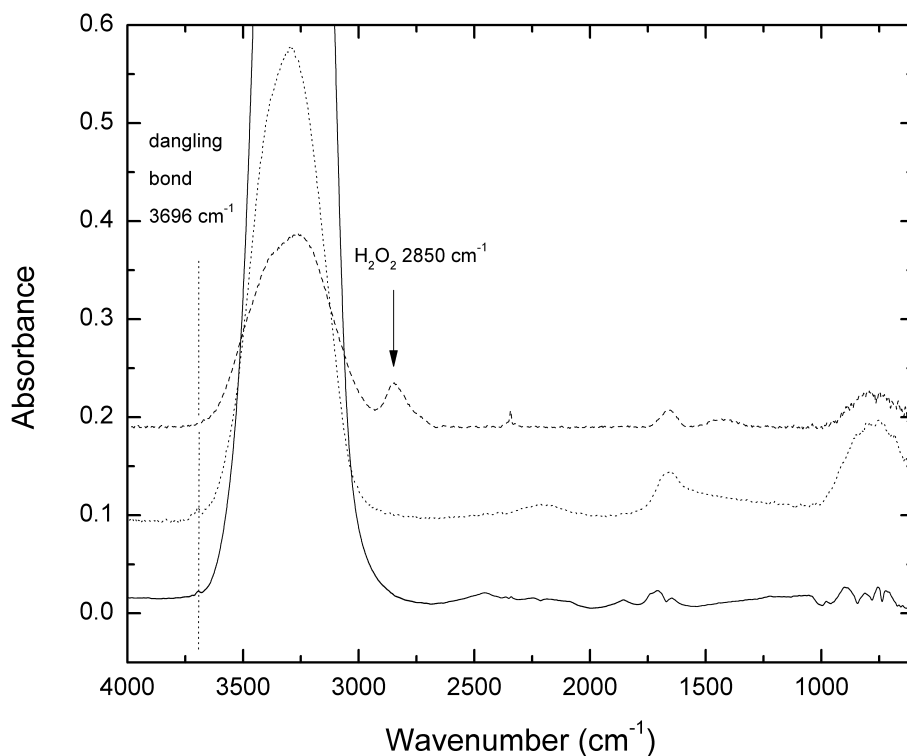


Figure 3.9: Spectra of deposited water at 2 torr for pure water (solid line), discharged pure water (dotted line), and discharged H<sub>2</sub>O:He 1:10 (dashed line) all at 6K.

Figure 3.9 shows that water discharged without a rare gas, does not produce any detectable H<sub>2</sub>O<sub>2</sub>. The discharged deposition of H<sub>2</sub>O:He mixtures produced a good amount of peroxide at 2850 cm<sup>-1</sup> even at 6K. At this deposition temperature, it is apparent that most OH produced end up forming H<sub>2</sub>O<sub>2</sub> and further experiments showed that most of the OH formed are via singlet oxygen. There is enough evidence to conclude that OH radicals cannot be trapped in thin water ice film. There is a contradiction between these results and that of another group performing similar experiments and will be covered in detailed in the discussion.

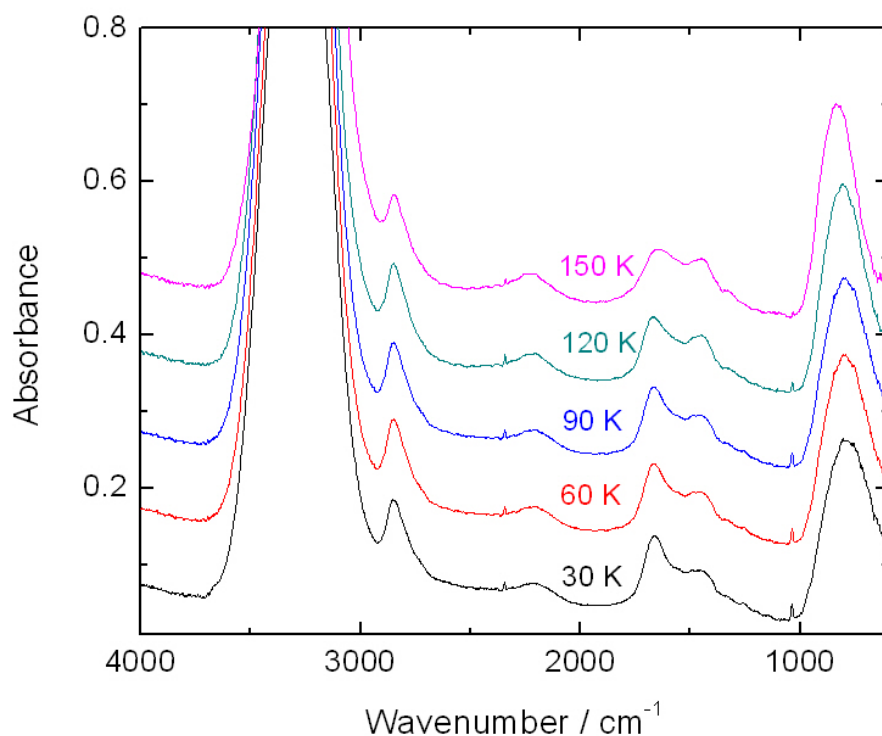


Figure 3.10: Deposition at 30K and warmed up to 150K in 30K interval.

The reason  $O_3$  is not present on depositions 60K and above is because it sublimates at 60K [28]. Figure 3.10 shows the remarkable stability of  $H_2O_2$  and  $O_3$  when deposited at 30K and warmed to 150K. This is significant since this trend has never been observed before in irradiated ice experiments. The presence of ozone is a strong evidence for molecular oxygen. Figure 3.11 shows the effect of warming a 30K and a 60K spectrum up to 150 at 30K intervals. This experiment explains the thermal properties of two OH radicals trapped in the same cage. When the sample is deposited at 30K, the low temperature prevents OH radicals from becoming mobile and escape the cage, therefore, most of the OH are reacted to form  $H_2O_2$  and very little are trapped. At 60K, OH have enough thermal energy to become mobile and escape the cage, allowing a greater percentage to be trapped, and upon warming, the trapped OH are released and destruction of  $H_2O_2$  follows. This is the reason

why we see a bigger drop in  $\text{H}_2\text{O}_2$  when the 60K sample is warmed compared to the 30K sample. This is also consistent with irradiated ice experiments.

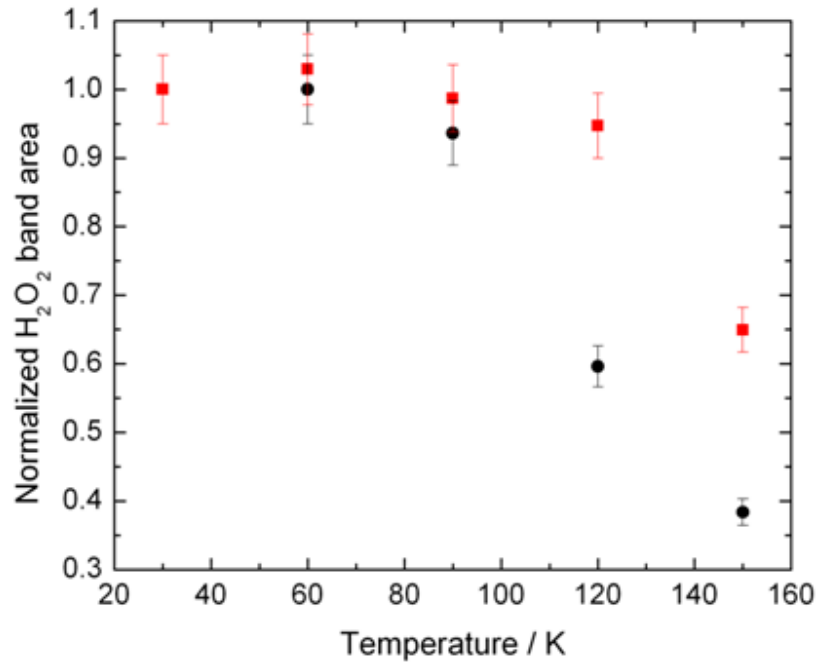


Figure 3.11: Dependence of normalized  $\text{H}_2\text{O}_2$  absorption band area upon warming of ice samples deposited at 30 K (red squares) and 60 K (black circles).

Qualitatively,  $O_2$  is shown to be present in the ice. As it is IR forbidden, direct quantitative determination in the ice is a challenge. The forbidden vibration mode of  $O_2$  at  $1550\text{ cm}^{-1}$  [12] is not present in the spectra, however, thermal program desorption experiments shows molecular oxygen mass peak at 32 amu (Figure 3.12). The big peak shown is due to sublimation of  $O_2$  at around 50K. A phase change occurs at around 150K where some trapped  $O_2$  is released. At 175K, sublimation of the  $H_2O$  sample occurred and just above this peak ( $\sim 180\text{K}$ ) could be due to released of trapped  $H_2O_2$ . Mass spectrometry cannot be use for quantitative analysis since  $H_2O_2$  is known to decompose into  $O_2$  when in contact with the stainless steel wall of the vacuum chamber.

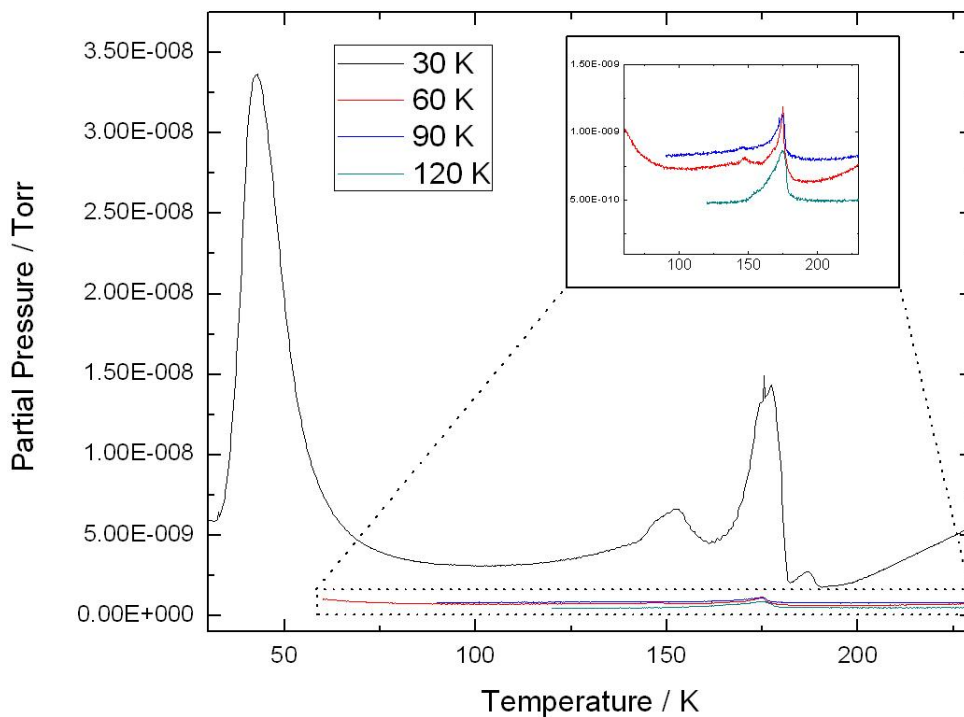


Figure 3.12: TPD (Mass 32) of ice deposited at 30K, 60K, 90K, and 120K.

UV spectra were obtained in hope to quantify  $O_2$  present in the ice, however, the pair of bands at  $\sim 575$  nm and  $\sim 627$  nm were not present in any of the redeposition experiments. These bands arise from the interaction of two  $O_2$  dimers, and as the ice is diluted, detection is impossible with the current instruments. Deposition of known amount of  $O_2$  (Figure 3.13) shows that at below 2 torr the peaks become indistinguishable from the background noise. Using an A-value of  $1.1 \times 10^4$  cm-molecule $^{-1}$  for  $O_2$  at 575 nm [77], the column density at 2 torr deposition was calculated to be  $4.5 \times 10^{16}$  molecule-cm $^{-2}$ , this value is three times the amount of  $O_3$  produced in the ice experiments. In order to make enough  $O_2$  for UV detection, the only way was to deposit for longer time but this had an undesirable consequence. Longer deposition made the ice sample too thick and opaque leading to very noisy, unreadable spectra.

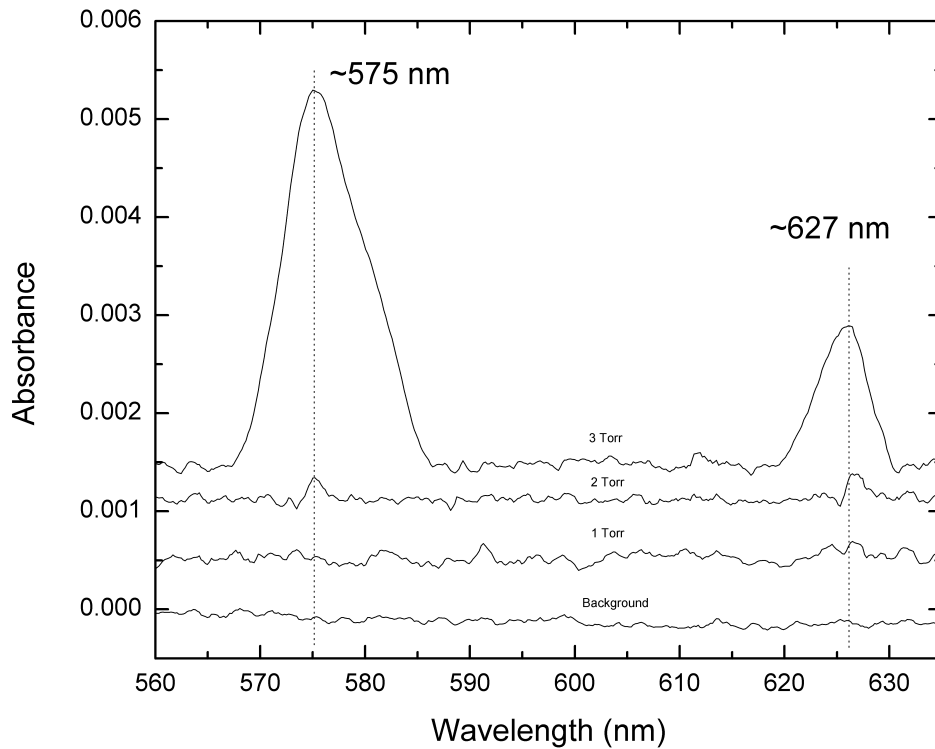


Figure 3.13: UV spectra of solid  $O_2$

To investigate the role of O atoms in the formation of  $\text{H}_2\text{O}_2$  and  $\text{O}_3$ ,  $\text{O}_2$ :He were discharged deposited alongside non-discharged  $\text{H}_2\text{O}$ :He (1:100) as shown in Figure 3.14. Like the  $\text{H}_2\text{O}$ :RG discharged depositions, both  $\text{H}_2\text{O}_2$  and  $\text{O}_3$  are present, the former up to 80K and the latter at 40K. At this point; strong evidence points toward O-atoms as one of the main precursors responsible for the formation of  $\text{H}_2\text{O}_2$ , as will be discussed later. In addition to the  $\text{O}_3$  peak at  $1040\text{ cm}^{-1}$ , two new peaks are present at  $1259\text{ cm}^{-1}$  and  $1550\text{ cm}^{-1}$  that belong to  $\text{HO}_3$  and  $\text{O}_2$ , respectively. In the latter case sufficient  $\text{O}_2$  is present in a heterogeneous environment to slightly relax the IR selection rules and so the vibration becomes allowed.

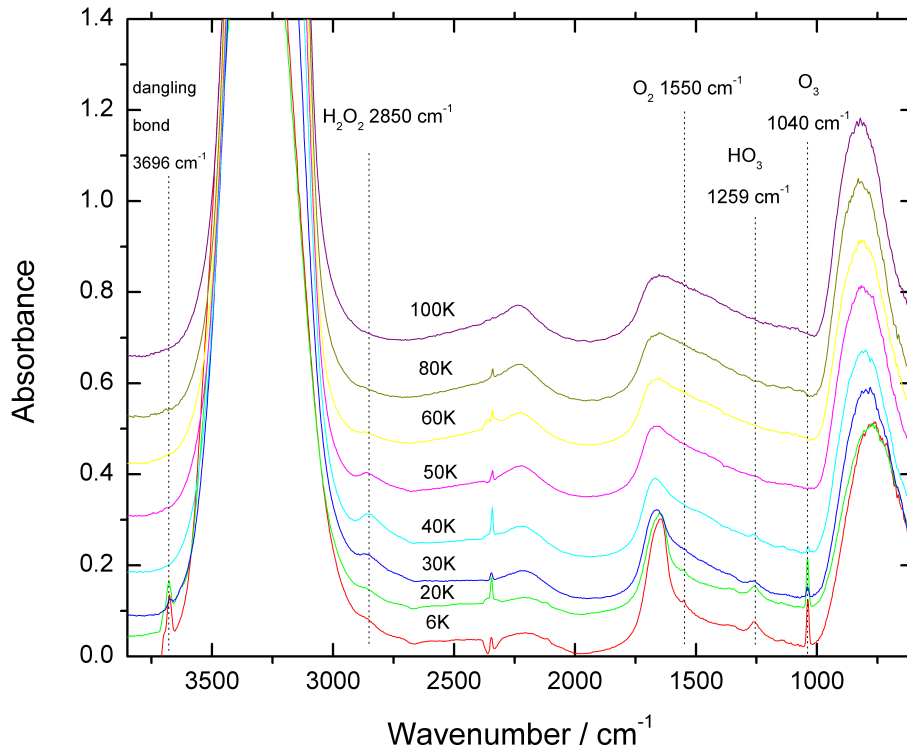


Figure 3.14: Co-deposition of  $\text{O}_2$ :He (discharged) and  $\text{H}_2\text{O}$ :He in 1:100 ratio at various temperatures.

Band area measurements of  $\text{H}_2\text{O}_2$  shows that its formation is greatest at 40K and goes down as the deposition temperature is lowered or increased (Figure 3.15)

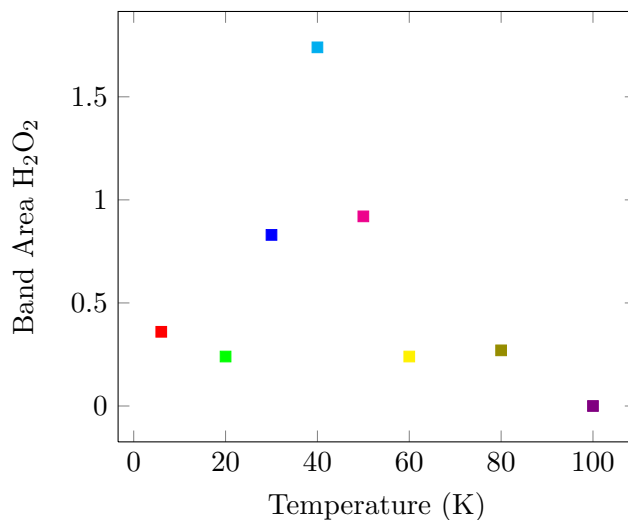


Figure 3.15: Band area of  $\text{H}_2\text{O}_2$  vs. deposition temperature.

$\text{HO}_3$  and  $\text{O}_3$  are favored at lower temperatures and become undetectable above 40K. The forbidden  $\text{O}_2$  absorption is only seen at low temperatures (below 20K). In these co-deposition experiments, there is a correlation between the relative abundance of  $\text{O}_3$  and  $\text{H}_2\text{O}_2$  in the ice. From 6-20K, where  $\text{O}_3$  band areas are highest,  $\text{H}_2\text{O}_2$  band areas are lowest. However, above 40K there is a decrease of  $\text{H}_2\text{O}_2$  formation and no  $\text{O}_3$  or  $\text{HO}_3$  present. It has been shown that  $\text{O}_2$  degases from water ice at 40K [147], therefore, this process may be reducing the  $\text{H}_2\text{O}_2$  production. Diatomic gases have been shown to be trapped efficiently in micro-porous amorphous ice up to 110K [91]. It is also important to note that the dangling bond shoulder at  $3696\text{ cm}^{-1}$  [120] are present at both 6K and 20K  $\text{O}$ -atom depositions and coincides with the present of the forbidden IR absorption of  $\text{O}_2$ . The presence of the dangling OH bond suggests the ice is porous which could trap some  $\text{O}_2$  in micro-pores. The current challenged mentioned in this section makes it impossible for the quantitative measurement of  $\text{O}_2$ .

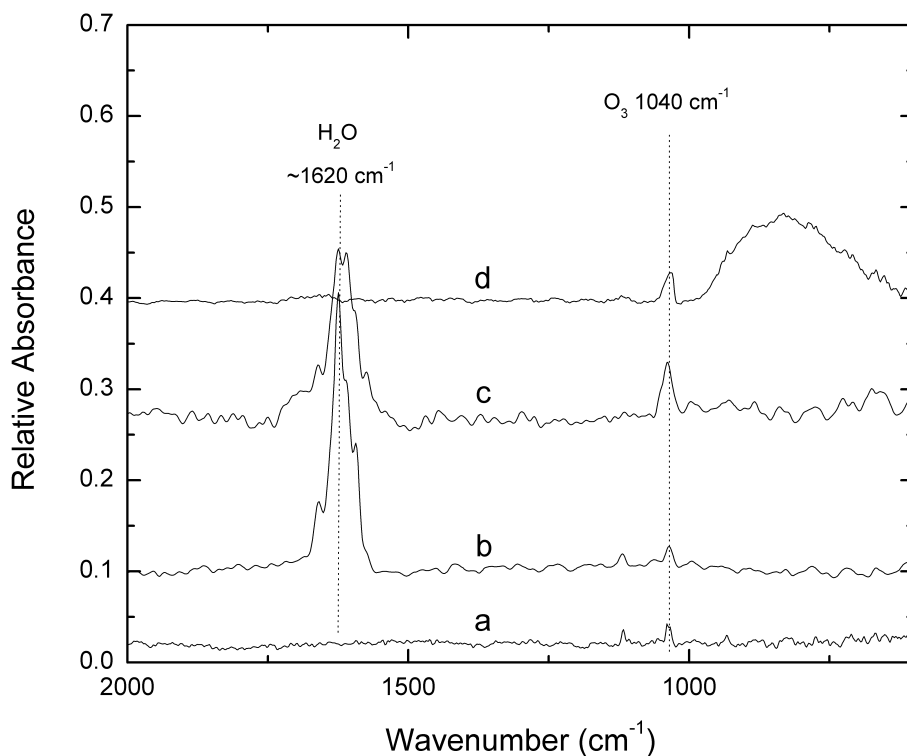


Figure 3.16: (a) O<sub>2</sub>:Ar discharged deposition at 6K, (b) H<sub>2</sub>O:Ar deposition on top of a, (c) layered warmed to 25K, (d) warmed to 40K.

Figure 3.16 shows the deposition of a layer of O atoms trapped in an argon matrix (a) and on top it a layer of H<sub>2</sub>O:Ar (1:100) was deposited soon after (b). It should be noted that singlet O atoms are known to efficiently relax back to the ground state triplet configuration in the rare gas matrices [121]. As seen from the spectra, O<sub>3</sub> is present in the 1040 cm<sup>-1</sup> at approximately the same band height before and after H<sub>2</sub>O:Ar was deposited. After warming up to 25K (c) and 40K (d), argon begins to sublime and reactions occur as a result of mixing producing more O<sub>3</sub>, as seen by the apparent increase in height of the 1040 cm<sup>-1</sup> peak. In the region from 4000 to 2400 cm<sup>-1</sup>, there is no absorption at 2850 cm<sup>-1</sup> for 3.17d, this mean H<sub>2</sub>O<sub>2</sub> was not produced as a result of the loss of the matrix and mixing

between triplet O atoms and H<sub>2</sub>O. When the matrix of H<sub>2</sub>O:Ar and O:Ar was warmed to 25K (Figure 3.17), and allowed to mix, evidently by more ozone production, there were no absorptions at 3450 cm<sup>-1</sup> and 3550 cm<sup>-1</sup> for free OH and H<sub>2</sub>O·HO, respectively. This imply that triplet O atoms do not react with water, since the reaction between O atoms and H<sub>2</sub>O (Eq. 1.4) will most likely produce H<sub>2</sub>O<sub>2</sub>, but we don't see any. The range of peaks between 4000 and 3200 cm<sup>-1</sup> corresponds to water clusters trapped in the argon matrix.

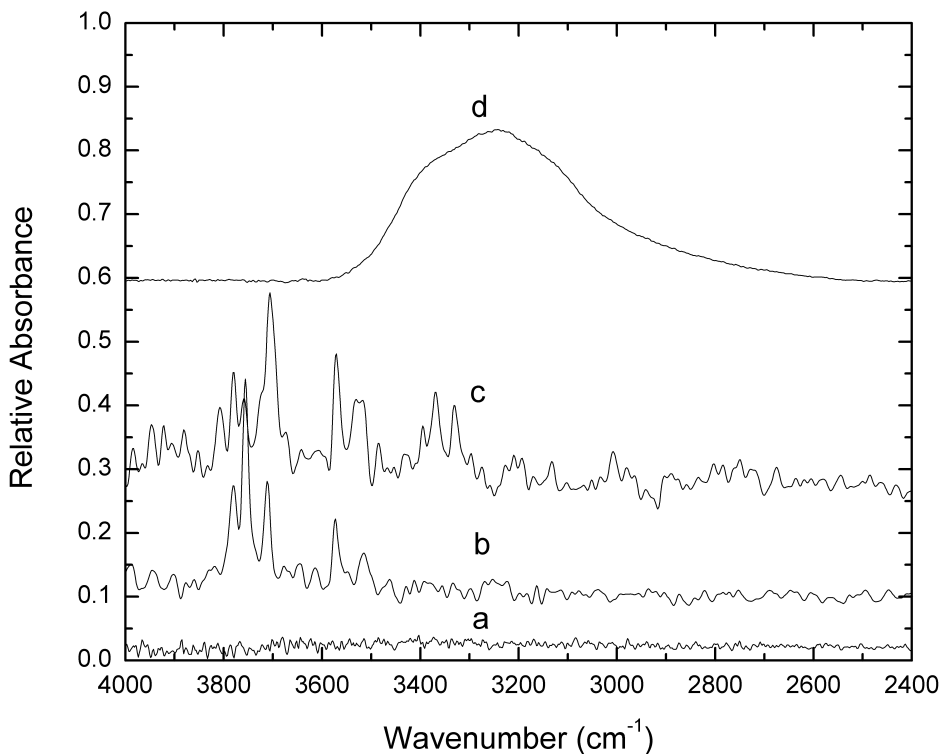


Figure 3.17: 4000 to 2400 cm<sup>-1</sup> spectra of (a) O<sub>2</sub>:Ar discharged deposition at 6K, (b) H<sub>2</sub>O:Ar deposition on top of a, (c) layered warmed to 25K, (d) warmed to 40K.

## 3.2 Discussions

There were three different experiments performed to help determine the role of radicals in water ice. The first was to determine the temperature dependence of oxidants formation by deposition of discharged H<sub>2</sub>O:RG mixtures (ice experiments). The second part was to show what radicals are produced in the discharge by matrix isolation techniques, in which only OH radicals could be quantitatively determined. Finally, the co-deposition of O<sub>2</sub>:RG (discharged) and H<sub>2</sub>O:RG (O atom experiments) in 1:1 ratio was to see if O atoms can initiate production of oxidants in the ice samples. In the following sections, analysis will be given on the chemistry that is occurring base on experimental results from these experiments and past traditional irradiated ice experiments.

### 3.2.1 Ice Experiments

The ice experiments show discharged depositions of H<sub>2</sub>O and rare gas vapor produces H<sub>2</sub>O<sub>2</sub> efficiently up to 60K. In addition, O<sub>3</sub> is also seen in the IR up to 50K. Matrix isolation experiments confirmed the following reactive species produced from the discharge: OH, HO<sub>2</sub>, and O atoms. The presence of O<sub>3</sub> is also a strong indication that O atoms are made by the discharge since its' formation is only possible by the reaction of a triplet oxygen atom (O(<sup>3</sup>P)) and molecular oxygen (O<sub>2</sub>). Based on past irradiation experiments, we know reactions between free OH radicals are the main pathway to production of H<sub>2</sub>O<sub>2</sub>, however, quantitation experiments of OH radicals does not agree with this conclusion. Therefore, in order to further understand this chemistry, an experiment where only O atoms (produced by O<sub>2</sub> discharge) are deposited with neutral water was done to determine if H<sub>2</sub>O<sub>2</sub> can be produced.

### 3.2.2 O Atom Experiments

In the O atom experiments, H<sub>2</sub>O<sub>2</sub> was produced up to 60K. This is interesting since H<sub>2</sub>O<sub>2</sub> formation from O atoms have never been observed before. O<sub>3</sub> was produced in large amount at 6K and 20K but disappeared above 40K. There were two new peaks that

were not seen in the H<sub>2</sub>O-discharge experiments. It is important to look at the two different types O atoms - singlet and triplet O(<sup>3</sup>P) - in the formation of H<sub>2</sub>O<sub>2</sub>. At this point, there is no way to differentiate between the O(<sup>1</sup>S) and O(<sup>1</sup>D) singlet oxygen. Since singlet is relaxed to O(<sup>3</sup>P) in a matrix environment, a layered experiment can be performed to study its' properties. In this experiment, layers of O:Ar and H<sub>2</sub>O:Ar are deposited in 1:1 ratio at 6K. At this temperature, the ice is matrix isolated and upon warming to 40K, an increased in the 1040 cm<sup>-1</sup> band (O<sub>3</sub>) was observed. Given the lack of OH absorption in the pre-warmed matrix sample, there is a strong indication that O(<sup>3</sup>P) does not react with H<sub>2</sub>O. This suggests singlet oxygen is the most likely precursor to the formation of H<sub>2</sub>O<sub>2</sub> in these experiments.

### 3.2.3 Similar Experiments Different Results

OH and HO<sub>2</sub> radicals are important precursors to the oxidation chemistry of surface water ice. Therefore, it is most important if they can be isolated and identified in water ice films in the laboratory. The present work does not find any spectral evidence of OH or HO<sub>2</sub> in ice, despite their presence in the gas phase prior to deposition. OH infrared absorption in ice likely occurs in the same region as the strong water stretching region. However, there was detection of HO<sub>3</sub> in the O atom experiments. Both OH and HO<sub>2</sub> were only seen in matrix isolated experiments in this research. HO<sub>2</sub> and HO<sub>3</sub> has been isolated in H<sub>2</sub>O + O<sub>2</sub> irradiated ice [29] at 1142 cm<sup>-1</sup> and 1259 cm<sup>-1</sup>, respectively, and verified by isotopic substitution. OH was observed by UV and EPR measurements in flash photolysis [41] and pulse radiolysis [139] water ice experiments. Recently, there were observations of OH and HO<sub>2</sub> in ice [40, 158] but their results are not in agreement with this research and the literature. By depositing microwave discharged water vapor onto a cold substrate, Zins et al. [158] reported OH at 3560 cm<sup>-1</sup>, HO<sub>2</sub> at 3424 cm<sup>-1</sup>, OH(H<sub>2</sub>O) complexes at 3726, 3628 and 3689 cm<sup>-1</sup>. While the HO<sub>2</sub> assignment is in agreement with previous work [40], however, it does not agree with the more recent work of Cooper et al. [29]. The techniques

employed by Zins et al. are similar to this work but our results do not agree and in fact vastly differ. In Figure 3.9, spectra were recorded to the exact conditions from Zins et al. experiments. The only difference is the energy used for the discharge; they used microwave discharge compared to a tesla coil discharge in this experiment. Aside from the main water peak ( $3300\text{ cm}^{-1}$ ), the spectra recorded in this experiment only shows a dangling bond for water discharged and  $\text{H}_2\text{O}_2$  at  $2850\text{ cm}^{-1}$  when water is discharged with helium. No other peaks were observed that match the assignments for OH and  $\text{HO}_2$  by Zins et al. Our experiments showed production of  $\text{H}_2\text{O}_2$  in which they did not see. Since  $\text{H}_2\text{O}_2$  is a product of OH radicals, a lack of the  $\text{H}_2\text{O}_2$  band is a good indication for the lack of OH unless trapping occurs in water ice. Given their samples are thin; trapping would not be a factor.

Gerakines et al. [40] reported free OH absorptions at  $3453$  and  $3428\text{ cm}^{-1}$ . They also based their peak assignments on matrix isolation experiments at the time, which is not the same as ice experiments due to site effects produced by the matrix. Recent work [27] shows that free OH has an absorption at  $3550\text{ cm}^{-1}$  in argon matrix and that the bands at  $3452$  and  $3428\text{ cm}^{-1}$  are due to  $\text{H}_2\text{O}\cdot\text{HO}$ . The  $\text{H}_2\text{O}\cdot\text{HO}$  complex can be explained by site effect phenomenon in which two molecules occupying two different sites within the host matrix can have their vibrational frequencies shifted with respect to one another. This has only been observed in matrix isolated samples and not likely to be present in thin water ice samples. Furthermore, Gerakines et al. also capped their ice samples with argon to prevent background contamination, this may have led to a near surface matrix isolation of  $\text{H}_2\text{O}\cdot\text{HO}$ .

Zins et al. [158] claim that peaks at  $3560$ ,  $3628$ ,  $3726$  and  $3689\text{ cm}^{-1}$  originate from OH radicals stably trapped in water ice or  $(\text{H}_2\text{O})_n\text{-OH}$  species. For the  $3689\text{ cm}^{-1}$  band, their assignment is to a  $(\text{H}_2\text{O})_n\text{-OH}$  species in which OH is hydrogen-bonded with water in the ice lattice, while the  $3560\text{ cm}^{-1}$  band is assigned to free OH.  $3726$  and  $3628\text{ cm}^{-1}$  bands correspond to the asymmetric ( $\nu_1$ ) and symmetric ( $\nu_3$ ) stretching modes of water of  $\text{H}_2\text{O}\cdot\text{HO}$ . These assignments are incorrect based upon a number of chemical and spectroscopic arguments. Their assignment of  $\text{HO}_2$  at  $1101\text{ cm}^{-1}$  is also incorrect and it should be

at  $1142\text{ cm}^{-1}$  in water ice as confirmed by Cooper et al. [29].

Free OH probably does not exist in a water rich environment with strong hydrogen bonding networks. Since the binding energy of  $\text{H}_2\text{O}\cdot\text{HO}$  is higher than for  $\text{H}_2\text{O}\cdot\text{H}_2\text{O}$ , OH binds stronger as a hydrogen-bonded species to water than other water molecules. A crystalline sample in which all  $\text{H}_2\text{O}$  molecules are bound could prevent a water molecule from accepting the OH hydrogen bond. Given the amorphous nature of their ices, it is unlikely that OH could exist freely. If the band at  $3560\text{ cm}^{-1}$  is free OH radical then there should be another band red-shifted  $100\text{ cm}^{-1}$  corresponding to the O-H stretch of  $\text{H}_2\text{O}\cdot\text{HO}$  [27]. This O-H stretch is 35 times more intense than free OH. Since other  $\text{H}_2\text{O}\cdot\text{HO}$  complexes were identified that had lower intensity, why was this band not seen? The peaks at  $3726$  and  $3628\text{ cm}^{-1}$  are likely due to  $(\nu_1)$  and  $(\nu_3)$  stretching modes of water. These are in agreement with nitrogen matrix isolation experiments reported as  $3736$  and  $3638\text{ cm}^{-1}$  [109]. The  $3689\text{ cm}^{-1}$  absorption band is not of  $(\text{H}_2\text{O})_n\text{-OH}$  but belongs to a dangling bond of O-H stretching vibration of water [119] between  $3680$  and  $3700\text{ cm}^{-1}$ . Dangling bonds could form with increasing ice growth. Although the peak appeared only in discharged samples, their non-discharged ice could have lower porosity compared to the ice produced with discharged. In addition, they were depositing with increasing time and this may produce a more porous ice and not an ice with  $(\text{H}_2\text{O})_n\text{-OH}$ . The disappearance of the  $3689\text{ cm}^{-1}$  upon warming to  $35\text{K}$  may be due to re-arrangement of the ice lattice structure such as pore collapse. The formation and disappearance of the dangling bonds may be temperature dependent and that some of the rare gas could be trapped in the ice that promotes the dangling bond formation. Higher deposition temperature reduced the efficiency of the trapping. In this work, dangling bonds are present only when pure water is discharged deposited and not seen in  $\text{H}_2\text{O}:\text{He}$  mixtures but at  $3696\text{ cm}^{-1}$ , not  $3689\text{ cm}^{-1}$ . The  $3689\text{ cm}^{-1}$  band seen in ices by Zins et al. may be due to contamination by nitrogen gas [120]. They also argued that the  $\text{CO}_2$  peak in their samples is evidence for OH radicals,



but they do not provide a reason for why CO is present as an impurity in the vacuum chamber. CO<sub>2</sub>, however, is present as impurity in the discharged and seen in this work. Explanations for CO<sub>2</sub> presence could be from oxidation of a trace organic molecule, such as pump oil vapor or vacuum grease by OH or singlet oxygen. Zins et al. [158] also claimed that the lack of H<sub>2</sub>O<sub>2</sub> in their spectra shows that recombination of two OH radicals can instead produced H<sub>2</sub>O.



This pathway is unlikely to be dominant over H<sub>2</sub>O<sub>2</sub> formation and experiments from this work do not agree with this reasoning. However, if this equation is to be dominant then O<sub>2</sub> and O<sub>3</sub> should be readily produced as well. In this work, thin sample experiments did not yield any O<sub>3</sub>, but with thicker samples, O<sub>3</sub> is detected at 1040 cm<sup>-1</sup>. There are other reasons for the lack of H<sub>2</sub>O<sub>2</sub> in their samples such as low production of radicals in the discharge or that OH and H are dominantly producing more H<sub>2</sub>O than H<sub>2</sub>O<sub>2</sub>.

This section is included to bring into light some of the contradictions in laboratory studies of reactive species in water ice. It has been well documented that radicals such as OH and HO<sub>2</sub> are elusive and mobile even in interstellar-like ice. The task is more difficult due to reactions between water and radical species. This is further complicated by many variables such as ice porosity, temperatures, and sample thickness. The goal here is provide a thorough understanding of reactive species in ice and to correct any misinterpretation of data in the literature since water radicals are important intermediates in the chemical evolution of planetary and interstellar ices.

### 3.2.4 OH

H<sub>2</sub>O<sub>2</sub> formations can occur via several pathways,



The most obvious reaction is 3.3, where two OH radicals dimerize. However, UV measurements of OH radicals produced from the discharged place a number ratio of 1.5% of OH relative to H<sub>2</sub>O. This number is much too low to produce the observed  $\sim 8\%$  of H<sub>2</sub>O<sub>2</sub> present in the ice. Since two OH radicals are needed to make one H<sub>2</sub>O<sub>2</sub>, the theoretical maximum should be  $\sim 0.75\%$ . There must be other pathways where H<sub>2</sub>O<sub>2</sub> is formed. OH can also react with H<sub>2</sub>O<sub>2</sub> to form HO<sub>2</sub>



which has been shown to occur in irradiated experiments [28]. When a 30K sample is warmed to 150K (Figure 3.10), there was no significant change to the H<sub>2</sub>O<sub>2</sub> peak. If there are trapped OH radicals in the ice, when warmed, it should react with H<sub>2</sub>O<sub>2</sub> to form HO<sub>2</sub>. OH radicals are known to be trapped in water ice at low temperatures and mobile around 80K. Since OH concentration is low compare to that of water in the samples, it is expected some OH must be trapped in the ice due to hydrogen bonding. However, these experiments suggest OH produced in the discharged are mobile on the surface below 30K and completely consumed by reactions. The ice samples are non-porous, due to the lack of the dangling bond, could also explain why there are no or little OH trapped. Since OH cannot account for all the H<sub>2</sub>O<sub>2</sub> produced, there must be another source.

### 3.2.5 HO<sub>2</sub> and HO<sub>3</sub>

HO<sub>2</sub> and HO<sub>3</sub> are seen in ice and matrix isolated experiments in the IR. HO<sub>2</sub> and HO<sub>3</sub> has only been observed in proton irradiated H<sub>2</sub>O + O<sub>2</sub> ice mixtures and irradiated H<sub>2</sub>O<sub>2</sub> ices [28]. Reactions 3.5 and 3.6 could also produce H<sub>2</sub>O<sub>2</sub>. At the present, there is no published A-value for the HO<sub>2</sub> absorptions at the 3412 cm<sup>-1</sup> band. In addition, UV measurements I performed do not show an absorption band at 205 nm [2]. Therefore, quantitative measurements of this radical are not possible at this time. However, it can be deduced from the absence of IR absorption of HO<sub>2</sub> in the ice experiments, small amounts may have been produced and most converted to form H<sub>2</sub>O<sub>2</sub> via the reactions above. Before we dive into the role of HO<sub>2</sub> in H<sub>2</sub>O<sub>2</sub> formation, I would like to discuss a few possible routes where HO<sub>2</sub> can be formed base on these experimental results. HO<sub>2</sub> formation can occur via the reactions,



and



It is likely that O<sub>2</sub> formed in the gas phase may react with H atoms and there is evidence in irradiated experiments that it does occur via eq 3.8 [29]. In the O atom experiments, there were no H atoms produced and HO<sub>2</sub> was also not present. However, HO<sub>3</sub> was observed, in significant amount at 6K and 20K. These evidence points to another pathway in which HO<sub>2</sub> and HO<sub>3</sub> is formed. HO<sub>3</sub> can be produced via,



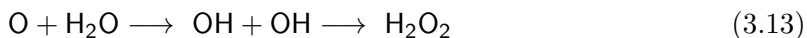
or



and that both reactions 3.8 and



are unlikely in the O atom experiments, due in part to the absence of H radicals. If any HO<sub>2</sub> were produced, it is plausible to explain its' formation via eq 3.9 since it is well-known that singlet oxygen can react with H<sub>2</sub>O to form two OH radicals, depending on the dilution of the ice, it may react to form H<sub>2</sub>O<sub>2</sub> or become trapped in the ice.



Subsequently, trapped OH may react with singlet oxygen to form HO<sub>2</sub>. As for HO<sub>3</sub>, it is unclear if eq 3.10 or eq 3.11 is the main pathway. Since, there were no H atoms produced and HO<sub>2</sub> were also not observed in the O atom experiments, it is difficult to argue that eq 3.10 is a contributor to HO<sub>3</sub> formation. In the ice experiments, HO<sub>2</sub> was indeed present, but HO<sub>3</sub> was never detected both in the UV or IR. However, with high concentration of O<sub>2</sub> in the O atom experiments, there was also high amount of HO<sub>3</sub> present. This leads to the implication of HO<sub>3</sub> formation via eq 3.11. In the O atom experiments, H<sub>2</sub>O and O<sub>2</sub> were deposited at ~1:1 ratio. At this concentration, O<sub>2</sub> is in a much greater abundance compared to the ice experiments. This creates an ice lattice rich in O<sub>2</sub>. Base on this model, OH radicals - produced by singlet oxygen - have a lower energy barrier to react with O<sub>2</sub> to form HO<sub>3</sub>. Potential energy surface calculations showed that in the ground state, eq 3.11 does not occur to any extend [146, 155] due to the energy of the HO<sub>3</sub> being lower than that of OH + O<sub>2</sub>. However, when O<sub>2</sub> and OH is in highly excited vibrational states, they are more likely to occur. In this scenario, OH produced by singlet oxygen is in a highly excited vibrational state. Studies have shown that vibrationally excited OH is relaxed in the presence of O<sub>2</sub> [36, 92]. Perhaps, this process occurred in the ice sample at low temperatures which also increased the chance of reaction between the two species to form HO<sub>3</sub>. This is also the first time that HO<sub>3</sub> is experimentally observed to be produced via this pathway. Previous work in irradiated ice experiments show that HO<sub>3</sub> is formed

via eq 3.12. To conclusively determine the formation pathway of HO<sub>3</sub>, more work must be done. The detection of HO<sub>3</sub> in the O atom experiments was interesting and unexpected, however, it may not provide us with any useful information regarding HO<sub>2</sub> on the formation of H<sub>2</sub>O<sub>2</sub> if their formations are not dependent on one another. The reactions between two HO<sub>2</sub> radicals may form H<sub>2</sub>O<sub>2</sub> according to eq 3.5. Also, HO<sub>2</sub> and an H atom can react to form H<sub>2</sub>O<sub>2</sub> via,



As mentioned earlier, it is not possible to quantify HO<sub>2</sub> at this time. In the ice experiments, there is no IR spectral evidence of HO<sub>2</sub>. This may suggest that eqs 3.5 and 3.14 are occurring to react away any deposited HO<sub>2</sub> to produce H<sub>2</sub>O<sub>2</sub>. This is likely, given the relatively high amount of H<sub>2</sub>O<sub>2</sub>. These reactions do not appear to occur in the matrix experiments, as evidenced by the lack of any measurable H<sub>2</sub>O<sub>2</sub>. Equation 3.5 is also a source of O<sub>2</sub>, which may then react with O(<sup>3</sup>P) to form O<sub>3</sub>. At least in the ice experiments, HO<sub>2</sub> is formed from the reaction between H and O<sub>2</sub>, either in the gas phase or soon after deposition (eq 3.8). Recently, it was shown that H<sub>2</sub>O<sub>2</sub> production is enhanced in irradiated ices when O<sub>2</sub> is present [28]. The explanation that O<sub>2</sub> produced in the gas phase reacting with H atoms to form HO<sub>2</sub> and subsequently producing H<sub>2</sub>O<sub>2</sub> is possible. There is a 2:1 H/O stoichiometric ratio in water and that H<sub>2</sub>O<sub>2</sub> is present at the ~8% by number relative to water, then there must be at least twice this percentage of H available if this reaction is to account for all H<sub>2</sub>O<sub>2</sub> production. However, HO<sub>2</sub> was not detected in the ice experiments, despite significant H<sub>2</sub>O<sub>2</sub>, it is plausible that eq 3.6 occurs much faster than eq 3.9. In other words, any HO<sub>2</sub> produced is immediately destroyed to make H<sub>2</sub>O<sub>2</sub>. In the O atom experiments, there is also no spectral evidence for HO<sub>2</sub>. In a diluted ice sample, like OH, there should be some amount of HO<sub>2</sub> trapped if it is produced.

### 3.2.6 O Atom

Radio frequency discharge of water vapor has been shown to produce reactive O atoms [106], as infer in these experiments indirectly by the present of O<sub>3</sub>. However, the total amount of O atoms produced is not known or measureable due to the lack of IR/UV absorptions. Predominantly, singlet oxygen, are formed in the discharged. This is the reason why O<sub>3</sub> is seen in the ice experiments but not the matrix isolated experiments. Either in the gas-phase or after deposition onto the substrate, two O(<sup>3</sup>P) may react to form O<sub>2</sub>,



consequently, O<sub>3</sub> may be formed from the reaction of triplet oxygen atoms O(<sup>3</sup>P) with O<sub>2</sub>.



The energetic discharge of an O<sub>2</sub> molecule or H<sub>2</sub>O (yields H<sub>2</sub> + O) also produces singlet oxygen. It may react in the gas phase to form O<sub>2</sub> and upon hitting the ice surface, some of the un-reacted O atoms are de-excited to O(<sup>3</sup>P) - and dependent on the temperature and ice properties - it may be trapped or react with O<sub>2</sub> to form O<sub>3</sub>. O(<sup>3</sup>P) is a product of the discharge and not from any surface reactions. The enhanced concentration of O<sub>3</sub> in the ice experiments suggest that enhanced production of O<sub>2</sub> in the ice, possibly due to eq 3.5 may be responsible. Singlet oxygen is also a source for OH radicals.



As shown in the O atom deposition experiments, H<sub>2</sub>O<sub>2</sub> is formed in significant amount and is consistent with eq 3.17. In matrix isolated experiments, singlet oxygen is quenched by the surrounding matrix to O(<sup>3</sup>P) [121] and was observed as the H<sub>2</sub>O·O(<sup>3</sup>P) complex [107]. O(<sup>3</sup>P) atoms may also be produced in the gas phase and complex with H<sub>2</sub>O upon deposition. However, the branching ratio of O(<sup>3</sup>P) to singlet produced by the discharge

is unknown. Another possibility that may account for  $O(^3P)$  is the reaction between two OH radicals, as seen in photolysis of  $H_2O_2$  ice [107]. If this process is occurring in these experiments then we would at least see some  $H_2O_2$  produced in the matrix experiments since two OH radicals are also bound to make  $H_2O_2$ . In the ice experiments, where the water density is much higher compare to matrix experiments, singlet oxygen have a much better chance of reacting with a water molecule before being quenched. This may be the reason why there are no  $H_2O_2$  present in matrix isolated experiments. Reactions are control by either the concentrations of water molecules or singlet oxygen. In the  $H_2O$  discharge experiments, there is a lack of  $O_3$  absorptions in the IR above 40-50K, this can be explain by the sublimation of  $O_2$ .  $O_2$  is volatile and does not absorb well in water ice. It has been shown that  $O_2$  is trapped in water ice at 27K and diffuses out of the ice at above 40K [147]. Vapor depositions of ice at high temperatures (60-150K) causes structural changes which may affect reactions of radicals [62]. Even at higher temperatures (60-80K), singlet oxygens are still able to produce  $H_2O_2$  however,  $O_2$  are being sublime before it could react with  $O(^3P)$  to form  $O_3$ . This was also observed in O atom deposition experiments.

$O(^3P)$  is also shown to be trapped in argon matrix and subsequent formation of  $O_3$  was observed in the bi-layer thermal experiments (Figure 3.16). When trapped  $O(^3P)$  is warmed in a bi-layer ice sample consisting of  $O(^3P)$  and  $H_2O$  in argon matrix (Figure 3.16c),  $O_3$  formation increased significantly. The degassing of argon atoms causes the matrix to collapse releasing  $O(^3P)$  which reacts with trapped  $O_2$  to yield  $O_3$ . However, when warmed to 40K (Figure 3.16d), the ozone concentration decreases slightly, this suggests  $O_2$  also sublimes from the sample at this temperature to reduce the  $O_3$  in the ice sample. This also imply that  $O(^3P)$  is not involved in the formation of  $H_2O_2$ . This is proven by the absence of  $H_2O_2$  at  $2850\text{ cm}^{-1}$  when the bi-layer sample is warmed to 40K, where  $H_2O_2$  is known to be in its greatest concentration. This also suggest that singlet oxygen can also be quenched to  $O(^3P)$  in the absence of a rare gas matrix.

The detection of  $H_2O \cdot O(^3P)$  in the matrix experiments support the idea that singlet

oxygen may be quenched and complex with  $\text{H}_2\text{O}$ . It is also possible that  $\text{O}(^3\text{P})$  may be produced in the discharge and complex with  $\text{H}_2\text{O}$  upon deposition. There is also evidence that two OH radicals can combine to form the  $\text{H}_2\text{O}\cdot\text{O}(^3\text{P})$  complex in a matrix as seen in the photolysis of  $\text{H}_2\text{O}_2$  [107]. If the latter process was occurring, depending on the orientation of the two OH radicals, we would expect to see some  $\text{H}_2\text{O}_2$  produced, however, it was not observed in the matrix experiment.

If eq 3.17 is mainly responsible for OH generation and relies on trapping of the subsequently produced OH radicals to form  $\text{H}_2\text{O}_2$ , then an increase in deposition temperature would enhance the escape of OH radicals and reduce the amount of  $\text{H}_2\text{O}_2$ . This would also increase the amount of OH trapped in the ice and upon warming would react and destroy  $\text{H}_2\text{O}_2$ . This was observed when 30K and 60K samples were both warmed to 150K at 30K interval (Figure 3.11). When the 30K sample was warmed to 150K, the relative amounts of  $\text{H}_2\text{O}_2$  remain almost unchanged. This implies that most of the OH were converted to  $\text{H}_2\text{O}_2$  and almost none are trapped. When the 60K sample was warmed to 150K, there was a clear decrease of  $\text{H}_2\text{O}_2$ . At the higher temperature, OH have enough thermal energy to escape the OH-OH cage to be freely trapped leading to  $\text{H}_2\text{O}_2$  destruction when warmed. This thermal behavior is consistent with singlet oxygen as the significant source of OH and ultimately  $\text{H}_2\text{O}_2$  in the ice experiments.

### 3.2.7 Impact of this Work

Part of the content of this research was recently published in the Journal of Physical Chemistry A [35]. A second manuscript has been submitted clarifying the identification of OH in water ice in response to the paper by Zins et al. and there is also a manuscript in preparation describing the role of O-atoms. The contribution of this work to the study of reactive species is significant. This is the first time that singlet oxygen is seen as the dominant precursor to the formation of  $\text{H}_2\text{O}_2$ . Even though there are many questions yet to be answered on the formation of oxidants from these experiments, this work serves as a platform for future research and it also opened a new door into the study of radicals in water

ice. Given that in irradiation experiments, only the products could be observed and the reaction intermediates can only be assumed since it is not observable in ice samples. This method of looking at radicals could provide invaluable insight on radiation products. Although the energy input into the sample is different from traditional experiments, however, the resulting ice samples are very similar. Given that radiolysis and photolysis experiments can differ greatly in product formations. There are so many things we have yet to learn about the chemistry of radicals in water ice and I believe this novel method can be useful for studying many other volatiles such as simple organic compounds.

### 3.3 Conclusion

We learned from these experiments that OH can be a source for H<sub>2</sub>O<sub>2</sub> production but quantitative data shows O atoms, specifically, singlet oxygen, is the dominant precursor. However, to account for this difference there must be a way to quantify the amount of O atoms in the sample. Currently, instrument limitations and the lack of an A value for O atoms inhibit this process. Another important observations was that HO<sub>3</sub> was produced in the discharged of O atom experiments. This has only been observed in irradiated H<sub>2</sub>O:O<sub>2</sub> ice mixtures. This shows the important chemistry is shared between these experiments and irradiated ice samples. There is a wealth of information that can be obtained from these experiments. Instead of using just H<sub>2</sub>O in the discharged, one could add SO<sub>2</sub> to study the formation pathways of sulfates in ice which is relevant to icy satellites [95, 96]. Future experiments could look into the thermal effects of O atoms in the reactions with H<sub>2</sub>O. This could provide interesting information on the role of O<sub>2</sub> and H<sub>2</sub>O<sub>2</sub> from sources to sinks for OH and O atoms. Proton irradiation experiments have only observed H<sub>2</sub>O<sub>2</sub>, and O<sub>2</sub> only seen in electron irradiation of water ice. In these experiments, both oxidants were observed and the chemistry for the most part is in good agreements with irradiation experiments.

These experiments provide important experimental information on the formation pathways of oxidants from reactive species. Like traditional experiments, the present experiments may allow us to better understand the chemical evolution of molecular species of

interests to icy surface of planetary bodies or satellites. The advantage is that if we could quantify the number of radicals produced, we could better understand the chemical processes in ice chemistry. These experiments also show that it doesn't matter what the source of radiation is, as long as there is a source of radicals, oxidants are formed in water ice. I believe this model can be applied to any ice surfaces where radicals are produced either in the laboratory or on the surfaces of outer solar system bodies.

The use of experimental techniques to study reactions in ice is a complicated task, since quantitative measurements are not always attainable. Therefore, we must rely heavily on the literature, past and current studies, to help in our understanding of the chemistry of radicals in ice. This is a delicate area of research in which we know very little about and care must be use when attempting to describe the chemistry. Whatever methods it may be, the common goal is to understand the chemistry in irradiated surface ice.

## Bibliography

- [1] N. Acquista, L. J. Schoen, and D. R. Lide. Infrared spectrum of the matrix-isolated OH radical. *The Journal of Chemical Physics*, 48(4):1534, 1968.
- [2] S. Aloisio, Y. Li, and J. S. Francisco. Complete active space self-consistent field and multireference configuration interaction studies of the differences between the low-lying excited states of HO<sub>2</sub> and HO<sub>2</sub>-H<sub>2</sub>O. *The Journal of Chemical Physics*, 110(18):9017, 1999.
- [3] M. Bahri, Y. Tarchouna, N. Jadane, Z. Ben Lakhdar, and J. Flament. Ab initio study of the hydrogen abstraction reaction H<sub>2</sub>O<sub>2</sub>+OH→HO<sub>2</sub>+H<sub>2</sub>O. *Journal of Molecular Structure: THEOCHEM*, 664-665:229–236, Dec. 2003.
- [4] A. Bar-Nun, G. Herman, M. Rappaport, and Y. Mekler. Ejection of H<sub>2</sub>O, O<sub>2</sub>, H<sub>2</sub> and H from water ice by 0.5 to 6 keV H<sup>+</sup> and Ne<sup>+</sup> ion bombardment. *Surface Science*, 150(1):143–156, Feb. 1985.
- [5] R. A. Baragiola and D. A. Bahr. Laboratory studies of the optical properties and stability of oxygen on ganymede. *Journal of Geophysical Research*, 103(E11):25865–72, 1998.
- [6] C. Barth, C. Hord, A. I. F. Steward, W. R. Pryor, K. E. Simmons, and W. E. McClintock. Galileo ultraviolet spectrometer observations of atomic hydrogen in the atmosphere of Ganymede. *Geophysical Research Letters*, 24(17):2147–50, 1997.

- [7] J.-P. Borra, R. A. Roos, D. Renard, H. Lazar, A. Goldman, and M. Goldman. Electrical and chemical consequences of point discharges in a forest during a mist and a thunderstorm. *Journal of Physics D: Applied Physics*, 30(1):84–93, Jan. 1997.
- [8] Y. Bouteiller and J. Perchard. The vibrational spectrum of  $(\text{H}_2\text{O})_2$ : Comparison between anharmonic ab initio calculations and neon matrix infrared data between 9000 and 90  $\text{cm}^{-1}$ . *Chemical Physics*, 305(1-3):1–12, Oct. 2004.
- [9] H. S. Bridge, J. W. Belcher, A. J. Lazarus, J. D. Sullivan, R. L. McNutt, F. Bagenal, J. D. Scudder, E. C. Sittler, G. L. Siscoe, V. M. Vasyliunas, C. K. Goertz, and C. M. Yeates. Plasma observations near Jupiter: Initial results from Voyager 1. *Science*, 204(4396):987–991, June 1979.
- [10] M. E. Brown and R. E. Hill. Discovery of an extended sodium atmosphere around Europa. *Nature*, 380(6571):229–231, Mar. 1996.
- [11] W. Brown, L. Lanzerotti, J. Poate, and W. Augustyniak. “Sputtering” of ice by MeV light ions. *Physical Review Letters*, 40(15):1027–1030, Apr. 1978.
- [12] B. R. Cairns and G. C. Pimentel. Infrared spectra of solid alpha- and beta-oxygen. *The Journal of Chemical Physics*, 43(10):3432, 1965.
- [13] W. M. Calvin, R. E. Johnson, and J. R. Spencer.  $\text{O}_2$  on Ganymede: Spectral characteristics and plasma formation mechanisms. *Geophysical Research Letters*, 23(6):673, 1996.
- [14] R. Carlson, M. Anderson, R. Johnson, W. Smythe, A. Hendrix, C. Barth, L. Soderblom, G. Hansen, T. McCord, J. Dalton, R. Clark, J. Shirley, A. Ocampo, and D. Matson. Hydrogen peroxide on the surface of Europa. *Science*, 283(5410):2062–4, 1999.
- [15] R. W. Carlson. A tenuous carbon dioxide atmosphere on Jupiter’s moon Callisto. *Science*, 283(5403):820–821, Feb. 1999.

- [16] T. Cassidy and R. Johnson. Collisional spreading of Enceladus neutral cloud. *Icarus*, 209(2):696–703, Oct. 2010.
- [17] E. Catalano and R. H. Sanborn. On the infrared spectrum of hydrogen peroxide matrix-isolation studies of the system  $\text{H}_2\text{O}_2:\text{N}_2$  (II). *The Journal of Chemical Physics*, 38(9):2273, 1963.
- [18] J. Ceponkus, G. Karlström, and B. Nelander. Intermolecular vibrations of the water trimer, a matrix isolation study. *The Journal of Physical Chemistry A*, 109(35):7859–7864, Sept. 2005.
- [19] J. Ceponkus and B. Nelander. Water dimer in solid neon. far-infrared spectrum. *The Journal of Physical Chemistry A*, 108(31):6499–6502, Aug. 2004.
- [20] J. Ceponkus, P. Uvdal, and B. Nelander. Water tetramer, pentamer, and hexamer in inert matrices. *The Journal of Physical Chemistry A*, 116(20):4842–4850, May 2012.
- [21] G. Cernogora, C. Szopa, and L. Boufendi. Plasma laboratory simulations of Titans aerosols. volume 799, pages 69–78. AIP, 2005.
- [22] L. Chu and C. Anastasio. Formation of hydroxyl radical from the photolysis of frozen hydrogen peroxide. *The Journal of Physical Chemistry A*, 109(28):6264–6271, July 2005.
- [23] C. F. Chyba. Energy for microbial life on Europa. *Nature*, 403(6768):381–382, Jan. 2000. PMID: 10667778.
- [24] J. Cooper. Energetic ion and electron irradiation of the icy Galilean satellites. *Icarus*, 149(1):133–159, Jan. 2001.
- [25] J. Cooper, P. Cooper, E. Sittler, S. J. Sturmer, and A. M. Rymer. Old faithful model for radiolytic gas-driven cryovolcanism at Enceladus. *Planetary and Space Science*, 57(13):1607–20, 2009.

- [26] P. Cooper, R. Johnson, and T. Quickenden. A review of possible optical absorption features of oxygen molecules in the icy surfaces of outer solar system bodies. *Planetary and Space Science*, 51(3):183–192, 2003.
- [27] P. Cooper, H. Kjaergaard, V. Langford, A. J. McKinley, T. I. Quickenden, and D. P. Schofield. Infrared measurements and calculations on H<sub>2</sub>O·HO. *Journal of the American Chemical Society*, 125(20):6048–6049, May 2003.
- [28] P. Cooper, M. Moore, and R. Hudson. Radiation chemistry of H<sub>2</sub>O+O<sub>2</sub> ices. *Icarus*, 194(1):379–388, Mar. 2008.
- [29] P. D. Cooper, M. H. Moore, and R. L. Hudson. Infrared detection of HO<sub>2</sub> and HO<sub>3</sub> radicals in water ice. *The Journal of Physical Chemistry A*, 110(26):7985–7988, July 2006. PMID: 16805481.
- [30] P. D. Cooper, M. H. Moore, and R. L. Hudson. O atom production in water ice: Implications for O<sub>2</sub> formation on icy satellites. *Journal of Geophysical Research*, 115(E10), Oct. 2010.
- [31] R. A. Cox and J. P. Burrows. Kinetics and mechanism of the disproportionation of hydroperoxyl radical in the gas phase. *The Journal of Physical Chemistry*, 83(20):2560–2568, Oct. 1979.
- [32] D. P. Cruikshank, T. J. Jones, and C. B. Pilcher. Absorption bands in the spectrum of Io. *The Astrophysical Journal*, 225:L89, Oct. 1978.
- [33] J. Dalton, D. Cruikshank, K. Stephan, T. McCord, A. Coustenis, R. Carlson, and A. Coradini. Chemical composition of icy satellite surfaces. *Space Science Review*, 153(1-4):113–154, 2010.
- [34] J. Dalton, O. Prieto-Ballesteros, J. Kargel, C. Jamieson, J. Jolivet, and R. Quinn. Spectral comparison of heavily hydrated salts with disrupted terrains on europa. *Icarus*, 177(2):472–490, Oct. 2005.

- [35] N. H. Do and P. D. Cooper. Formation and reaction of oxidants in water ice produced from the deposition of RF-Discharged rare gas and water mixtures. *The Journal of Physical Chemistry A*, 117(1):153–159, Jan. 2013.
- [36] J. A. Dodd, S. J. Lipson, and W. A. M. Blumberg. Formation and vibrational relaxation of OH ( $X^2\Pi_{i,v}$ ) by O<sub>2</sub> and CO<sub>2</sub>. *The Journal of Chemical Physics*, 95(8):5752, 1991.
- [37] F. Du, B. Parise, and P. Bergman. Production of interstellar hydrogen peroxide (H<sub>2</sub>O<sub>2</sub>) on the surface of dust grains. *Astronomy & Astrophysics*, 538:A91, Feb. 2012.
- [38] P. Geissler, A. McEwen, C. Phillips, D. Simonelli, R. M. C. Lopes, and S. Dout. Galileo imaging of SO<sub>2</sub> frosts on Io. *Journal of Geophysical Research*, 106(E12):33253–33266, 2001.
- [39] P. Geissler and M. McMillan. Galileo observations of volcanic plumes on Io. *Icarus*, 197(2):505–518, Oct. 2008.
- [40] P. A. Gerakines, W. A. Schutte, and P. Ehrenfreund. Ultraviolet processing of interstellar ice analogs i. pure ices. *Astronomy Astrophysics*, 312:289–305, 1996.
- [41] J. A. Ghormley and C. J. Hochanadel. Production of hydrogen, hydroxide, and hydrogen peroxide in the flash photolysis of ice. *The Journal of Physical Chemistry*, 75(1):40–44, Jan. 1971.
- [42] O. Gomis, M. Satorre, G. Strazzulla, and G. Leto. Hydrogen peroxide formation by ion implantation in water ice and its relevance to the Galilean satellites. *Planetary and Space Science*, 52:371–378, 2004.
- [43] J. L. Grenfell, R. Lehmann, P. Mieth, U. Langematz, and B. Steil. Chemical reaction pathways affecting stratospheric and mesospheric ozone. *Journal of Geophysical Research*, 111(D17), 2006.

- [44] G. A. Grieves and T. M. Orlando. The importance of pores in the electron stimulated production of  $D_2$  and  $O_2$  in low temperature ice. *Surface Science*, 593(1-3):180–186, Nov. 2005.
- [45] P. Haff and A. Eviatar. Micrometeoroid impact on planetary satellites as a magnetospheric mass source. *Icarus*, 66(2):258–269, May 1986.
- [46] D. Hall, D. Strobel, P. Feldman, M. McGrath, and H. Weaver. Detection of an oxygen atmosphere on Jupiter’s moon Europa. *Nature*, 373:677–679, 1995.
- [47] E. J. Hamilton. Water vapor dependence of the kinetics of the self-reaction of  $HO_2$  in the gas phase. *The Journal of Chemical Physics*, 63(8):3682, 1975.
- [48] G. B. Hansen and T. B. McCord. Widespread  $CO_2$  and other non-ice compounds on the anti-Jovian and trailing sides of Europa from Galileo/NIMS observations. *Geophysical Research Letters*, 35(1), Jan. 2008.
- [49] S. Hirabayashi and K. M. Yamada. Infrared spectra and structure of water clusters trapped in argon and krypton matrices. *Journal of Molecular Structure*, 795(1-3):78–83, Aug. 2006.
- [50] S. Hirabayashi and K. M. Yamada. The monocyclic water hexamer detected in neon matrices by infrared spectroscopy. *Chemical Physics Letters*, 435(1-3):74–78, Feb. 2007.
- [51] R. B. Horne, R. M. Thorne, Y. Y. Shprits, N. P. Meredith, S. A. Glauert, A. J. Smith, S. G. Kanekal, D. N. Baker, M. J. Engebretson, J. L. Posch, M. Spasojevic, U. S. Inan, J. S. Pickett, and P. M. E. Decreau. Wave acceleration of electrons in the van allen radiation belts. *Nature*, 437(7056):227–230, Sept. 2005.
- [52] D. M. Hudgins, S. A. Sandford, L. J. Allamandola, and A. G. G. M. Tielens. Mid- and far-infrared spectroscopy of ices - optical constants and integrated absorbances. *The Astrophysical Journal Supplement Series*, 86:713, June 1993.

- [53] R. Hudson and M. Moore. Infrared spectra and radiation stability of H<sub>2</sub>O<sub>2</sub> ices relevant to Europa. *Astrobiology*, 6(3):483–489, 2006.
- [54] R. L. Hudson and M. H. Moore. A far-IR study of irradiated amorphous ice: an unreported oscillation between amorphous and crystalline phases. *The Journal of Physical Chemistry*, 96(15):6500–6504, July 1992.
- [55] R. L. Hudson and M. H. Moore. Far-IR spectral changes accompanying proton irradiation of solids of astrochemical interest. *Radiation Physics and Chemistry*, 45(5):779–789, May 1995.
- [56] W. Ip. Europa’s oxygen exosphere and its magnetospheric interaction. *Icarus*, 120(2):317–325, Apr. 1996.
- [57] W.-H. Ip, D. J. Williams, R. W. McEntire, and B. H. Mauk. Ion sputtering and surface erosion at Europa. *Geophysical Research Letters*, 25(6):829, Mar. 1998.
- [58] M. E. Jacox and D. E. Milligan. Spectrum and structure of the HO<sub>2</sub> free radical. *Journal of Molecular Spectroscopy*, 42(3):495–513, June 1972.
- [59] R. Johnson. Sodium at Europa. *Icarus*, 143(2):429–433, Feb. 2000.
- [60] R. Johnson and W. Jesser. O<sub>2</sub>/O<sub>3</sub> microatmospheres in the surface of Ganymede. *The Astronomical Journal*, 480:L79–L82, 1997.
- [61] R. Johnson, J. Luhmann, R. Tokar, M. Bouhram, J. Berthelier, E. Sittler, J. Cooper, T. Hill, H. Smith, and M. Michael. Production, ionization and redistribution of O<sub>2</sub> in Saturn’s ring atmosphere. *Icarus*, 180(2):393–402, Feb. 2006.
- [62] R. Johnson and T. Quickenden. Photolysis and radiolysis of water ice on the outer solar system bodies. *Journal of Geophysical Research*, 102(E5):10985–10996, 1997.
- [63] R. E. Johnson. *Energetic charged-particle interactions with atmospheres and surfaces*. Springer-Verlag, Berlin; New York, 1990.

- [64] R. E. Johnson. Sputtering and desorption from icy surfaces. In B. Schmitt, C. Bergh, and M. Festou, editors, *Solar System Ices*, volume 227, pages 303–334. Springer Netherlands, Dordrecht, 1998.
- [65] R. E. Johnson, P. D. Cooper, T. I. Quickenden, G. A. Grieves, and T. M. Orlando. Production of oxygen by electronically induced dissociations in ice. *The Journal of Chemical Physics*, 123(18):184715, 2005.
- [66] R. E. Johnson, R. M. Killen, J. H. Waite, and W. S. Lewis. Europa’s surface composition and sputter-produced ionosphere. *Geophysical Research Letters*, 25(17):3257, Sept. 1998.
- [67] R. E. Johnson, T. I. Quickenden, P. D. Cooper, A. J. McKinley, and C. G. Freeman. The production of oxidants in Europa’s surface. *Astrobiology*, 3(4):823–850, Dec. 2003.
- [68] R. E. Johnson and E. C. Sittler. Sputter-produced plasma as a measure of satellite surface composition: The CASSINI mission. *Geophysical Research Letters*, 17(10):1629, 1990.
- [69] S. Jurac. Saturn search for a missing water source. *Geophysical Research Letters*, 29(24), 2002.
- [70] K. Kamiyama, H. Motoyama, Y. Fujii, and O. Watanabe. Distribution of hydrogen peroxide in surface snow over Antarctic ice sheet. *Atmospheric Environment*, 30(6):967–972, Mar. 1996.
- [71] J. Kargel. Cryovolcanism on the icy satellites. *Earth, Moon, and Planets*, 67(1-3):101–13, 1995.
- [72] A. U. Khan and M. Kasha. Chemiluminescence arising from simultaneous transitions in pairs of singlet oxygen molecules. *Journal of the American Chemical Society*, 92(11):3293–3300, June 1970.

- [73] R. M. Killen, D. M. Hurley, and W. M. Farrell. The effect on the lunar exosphere of a coronal mass ejection passage. *Journal of Geophysical Research*, 117, Mar. 2012.
- [74] C. C. Kircher and S. P. Sander. Kinetics and mechanism of HO<sub>2</sub> and DO<sub>2</sub> disproportionations. *The Journal of Physical Chemistry*, 88(10):2082–2091, May 1984.
- [75] M. J. Kurylo, J. L. Murphy, G. S. Haller, and K. D. Cornett. A flash photolysis resonance fluorescence investigation of the reaction OH+H<sub>2</sub>O<sub>2</sub> → HO<sub>2</sub>+H<sub>2</sub>O. *International Journal of Chemical Kinetics*, 14(10):1149–1161, Oct. 1982.
- [76] J. J. Lamb, L. T. Molina, C. A. Smith, and M. J. Molina. Rate constant of the OH+H<sub>2</sub>O<sub>2</sub> → HO<sub>2</sub>+H<sub>2</sub>O. *The Journal of Physical Chemistry*, 87(22):4467–4470, Oct. 1983.
- [77] A. Landau, E. J. Allin, and H. Welsh. The absorption spectrum of solid oxygen in the wavelength region from 12,000 to 3300 angstrom. *Spectrochimica Acta*, 18:1–19, Jan. 1962.
- [78] A. L. Lane, R. M. Nelson, and D. L. Matson. Evidence for sulphur implantation in Europa’s UV absorption band. *Nature*, 292(5818):38–39, July 1981.
- [79] L. Lanzerotti, W. Brown, J. Poate, and W. Augustyniak. On the contribution of water products from Galilean satellites to the Jovian magnetosphere. *Geophysical Research Letters*, 5(2):155, 1978.
- [80] L. J. Lanzerotti, W. L. Brown, K. J. Marcantonio, and R. E. Johnson. Production of ammonia-depleted surface layers on the Saturnian satellites by ion sputtering. *Nature*, 312(5990):139–140, Nov. 1984.
- [81] L. J. Lanzerotti, D. C. Webb, and C. W. Arthur. Geomagnetic field fluctuations at synchronous orbit 2. radial diffusion. *Journal of Geophysical Research*, 83(A8):3866, 1978.

- [82] F. Leblanc, A. Potter, R. Killen, and R. Johnson. Origins of Europa Na cloud and torus. *Icarus*, 178(2):367–385, Nov. 2005.
- [83] L. Lebofsky. Identification of water frost on Callisto. *Nature*, 269(5631):785–787, Oct. 1977.
- [84] R.-R. Lii, M. C. Sauer, and S. Gordon. Temperature dependence of the gas-phase self-reaction of hydroperoxo in the presence of water. *The Journal of Physical Chemistry*, 85(19):2833–2834, Sept. 1981.
- [85] M. Loeffler, U. Raut, R. Vidal, R. Baragiola, and R. W. Carlson. Synthesis of hydrogen peroxide in water ice by ion irradiation. *Icarus*, 180:265–273, 2006.
- [86] M. J. Loeffler. The state of hydrogen peroxide on Europa. *Geophysical Research Letters*, 32(17), 2005.
- [87] M. J. Loeffler and R. A. Baragiola. Physical and chemical effects on crystalline H<sub>2</sub>O<sub>2</sub> induced by 20 keV protons. *The Journal of Chemical Physics*, 130(11):114504, 2009.
- [88] J. Luhmann, R. Johnson, R. Tokar, S. Ledvina, and T. Cravens. A model of the ionosphere of Saturn’s rings and its implications. *Icarus*, 181(2):465–474, Apr. 2006.
- [89] A. Mansergas and J. M. Anglada. The gas-phase reaction between O<sub>3</sub> and HO radical: A theoretical study. *ChemPhysChem*, 8(10):1534–1539, July 2007.
- [90] A. Mardyukov and W. Sander. Matrix isolation of radicals. In C. Chatgililoglu and A. Studer, editors, *Encyclopedia of Radicals in Chemistry, Biology and Materials*. John Wiley & Sons, Ltd, Chichester, UK, Mar. 2012.
- [91] E. Mayer and R. Pletzer. Astrophysical implications of amorphous ice a microporous solid. *Nature*, 319(6051):298–301, Jan. 1986.
- [92] D. McCabe, I. Smith, B. Rajakumar, and A. Ravishankara. Rate coefficients for the

- relaxation of OH ( $v=1$ ) by O<sub>2</sub> at temperatures from 204-371K and by N<sub>2</sub>O from 243-372K. *Chemical Physics Letters*, 421(1-3):111–117, Apr. 2006.
- [93] T. R. McDonough. Jupiter after Pioneer: A progress report. *Nature*, 251:17–20, 1974.
- [94] M. Moore and R. Hudson. IR detection of H<sub>2</sub>O<sub>2</sub> at 80 K in ion-irradiated laboratory ices relevant to Europa. *Icarus*, 145(1):282–288, May 2000.
- [95] M. Moore, R. Hudson, and R. Carlson. The radiolysis of SO<sub>2</sub> and H<sub>2</sub>S in water ice: Implications for the icy Jovian satellites. *Icarus*, 189(2):409–423, Aug. 2007.
- [96] M. H. Moore. Studies of proton-irradiated SO<sub>2</sub> at low temperatures: Implications for Io. *Icarus*, 59(1):114–128, July 1984.
- [97] D. B. Nash, F. P. Fanale, and R. M. Nelson. SO<sub>2</sub> frost: UV-visible reflectivity and Io surface coverage. *Geophysical Research Letters*, 7(9):665, 1980.
- [98] R. M. Nelson and W. D. Smythe. Spectral reflectance of solid sulfur trioxide (0.25-5.2 micron): Implications for Jupiter’s satellite Io. *Icarus*, 66(1):181–187, Apr. 1986.
- [99] G. Nilsson, H. C. Christensen, J. Fenger, P. Pagsberg, and S. O. Nielsen. Pulse radiolysis of ice and frozen hydrogen fluoride solutions. *Advances in Chemistry Series*, 81:71–78, 1968.
- [100] K. Noll. 3- to 13-micron spectra of Io. *Icarus*, 104(2):337–340, Aug. 1993.
- [101] K. Noll, R. Johnson, A. Lane, D. Domingue, and H. Weaver. Detection of ozone on Ganymede. *Science*, 273(5273):341–343, July 1996.
- [102] K. S. Noll, R. E. Johnson, M. A. McGrath, and J. J. Caldwell. Detection of SO<sub>2</sub> on Callisto with the Hubble space telescope. *Geophysical Research Letters*, 24(9):1139, 1997.

- [103] K. S. Noll, T. L. Roush, D. P. Cruikshank, R. E. Johnson, and Y. J. Pendleton. Detection of ozone on Saturn's satellites Rhea and Dione. *Nature*, 388(6637):45–47, July 1997. PMID: 9214500.
- [104] T. M. Orlando and M. Sieger. The role of electron-stimulated production of O<sub>2</sub> from water ice in the radiation processing of outer solar system surfaces. *Surface Science*, 528(1-3):1–7, Mar. 2003.
- [105] G. S. Orton, J. R. Spencer, L. D. Travis, T. Z. Martin, and L. K. Tamppari. Galileo photopolarimeter-radiometer observations of jupiter and the galilean satellites. *Science*, 274(5286):389–391, Oct. 1996.
- [106] M. P. Pearce, M. J. Bussemaker, P. D. Cooper, K. M. Lapere, D. A. Wild, and A. J. McKinley. Formation of methanol from methane and water in an electrical discharge. *Physical Chemistry Chemical Physics*, 14(10):3444, 2012.
- [107] S. Pehkonen, M. Pettersson, J. Lundell, L. Khriachtchev, and M. Rsnen. Photochemical studies of hydrogen peroxide in solid rare gases: Formation of the HOH-O(3P) complex. *The Journal of Physical Chemistry A*, 102(39):7643–7648, Sept. 1998.
- [108] S. A. Penkett, B. J. Bandy, C. E. Reeves, D. McKenna, and P. Hignett. Measurements of peroxides in the atmosphere and their relevance to the understanding of global tropospheric chemistry. *Faraday Discussions*, 100:155, 1995.
- [109] J. Perchard. Anharmonicity and hydrogen bonding. II. a near infrared study of water trapped in nitrogen matrix. *Chemical Physics*, 266(1):109–124, May 2001.
- [110] N. G. Petrik, A. G. Kavetsky, and G. A. Kimmel. Electron-stimulated production of molecular oxygen in amorphous solid water. *The Journal of Physical Chemistry B*, 110(6):2723–2731, Feb. 2006.
- [111] N. G. Petrik, A. G. Kavetsky, and G. A. Kimmel. Electron stimulated production of molecular oxygen in amorphous solid water on Pt precursor transport through the

- hydrogen bonding network. *The Journal of Chemical Physics*, 125(12):124702–1/11, 2006.
- [112] M. Pettersson, S. Tuominen, and M. Rsnen. IR spectroscopic study of H<sub>2</sub>O<sub>2</sub>, HDO<sub>2</sub>, and D<sub>2</sub>O<sub>2</sub> isolated in Ar, Kr, and Xe matrices. *The Journal of Physical Chemistry A*, 101(6):1166–1171, Feb. 1997.
- [113] C. Pilcher, S. Ridgway, and T. McCord. Galilean satellites: identification of water frost. *Science*, 178(4065):1087–9, 1972.
- [114] C. B. Pilcher. The stability of water in Io. *Icarus*, 37(3):559–574, Mar. 1979.
- [115] F. Postberg, E. Grn, M. Horanyi, S. Kempf, H. Krger, J. Schmidt, F. Spahn, R. Srama, Z. Sternovsky, and M. Tieloff. Compositional mapping of planetary moons by mass spectrometry of dust ejecta. *Planetary and Space Science*, 59(14):1815–1825, Nov. 2011.
- [116] A. Radioti. Ion abundance ratios in the Jovian magnetosphere. *Journal of Geophysical Research*, 110(A7), 2005.
- [117] S. Ramirez, P. Coll, and A. da Silva. Complex refractive index of Titan’s aerosol analogues in the 200-900 nm domain. *Icarus*, 156(2):515–529, Apr. 2002.
- [118] M. N. Ross and G. Schubert. Tidal heating in an internal ocean model of Europa. *Nature*, 325(6100):133–134, Jan. 1987.
- [119] B. Rowland and J. P. Devlin. Spectra of dangling OH groups at ice cluster surfaces and within pores of amorphous ice. *The Journal of Chemical Physics*, 94(1):812, 1991.
- [120] B. Rowland, M. Fisher, and J. P. Devlin. Probing icy surfaces with the dangling-OH-mode absorption: Large ice clusters and microporous amorphous ice. *The Journal of Chemical Physics*, 95(2):1378, 1991.

- [121] E. Ryan and E. Weitz. O atom photoproduction dynamics and reactions in cryogenic solids. *Chemical Physics*, 189(2):293–305, Dec. 1994.
- [122] N. Sack and R. Baragiola. Sublimation of vapor-deposited water ice below 170 K, and its dependence on growth conditions. *Physical Review B*, 48(14):9973–9978, Oct. 1993.
- [123] J. Saur, D. F. Strobel, and F. M. Neubauer. Interaction of the Jovian magnetosphere with Europa: Constraints on the neutral atmosphere. *Journal of Geophysical Research*, 103(E9):19947–19962, 1998.
- [124] D. E. Shemansky, P. Matheson, D. T. Hall, H.-Y. Hu, and T. M. Tripp. Detection of the hydroxyl radical in the Saturn magnetosphere. *Nature*, 363(6427):329–331, May 1993.
- [125] V. Shematovich and R. Johnson. Near-surface oxygen atmosphere at Europa. *Advances in Space Research*, 27(11):1881–1888, Jan. 2001.
- [126] V. Shematovich, R. Johnson, J. Cooper, and M. Wong. Surface-bounded atmosphere of Europa. *Icarus*, 173(2):480–498, 2005.
- [127] J. Shi, B. Teolis, and R. Baragiola. Irradiation-enhanced adsorption and trapping of O<sub>2</sub> on nanoporous water ice. *Physical Review B*, 79(23), June 2009.
- [128] T. Shimanouchi. Tables of molecular vibrational frequencies. consolidated volume II. *Journal of Physical and Chemical Reference Data*, 6(3):993, 1977.
- [129] V. N. Shubin, V. A. Zhigunov, V. I. Zolotarevsky, and P. I. Dolin. Pulse radiolysis of crystalline ice and frozen crystalline aqueous solutions. *Nature*, 212(5066):1002–1035, Dec. 1966.
- [130] M. Sieger, W. Simpson, and T. Orlando. Production of O<sub>2</sub> on icy satellites by electronic excitation of low-temperature water ice. *Nature*, 394(6693):554–6, 1998.

- [131] E. Sieveka and R. Johnson. Thermal- and plasma-induced molecular redistribution on the icy satellites. *Icarus*, 51(3):528–548, Sept. 1982.
- [132] A. Sigg and A. Neftel. Evidence for a 50 percent increase in H<sub>2</sub>O<sub>2</sub> over the past 200 years from a Greenland ice core. *Nature*, 351(6327):557–559, June 1991.
- [133] S. Solomon, R. R. Garcia, F. S. Rowland, and D. J. Wuebbles. On the depletion of Antarctic ozone. *Nature*, 321(6072):755–758, June 1986.
- [134] J. R. Spencer and W. M. Calvin. Condensed O<sub>2</sub> on Europa and Callisto. *The Astronomical Journal*, 124:3400–03, 2002.
- [135] J. R. Spencer, W. M. Calvin, and M. J. Person. Charge-coupled device spectra of the Galilean satellites: Molecular oxygen on Ganymede. *Journal of Geophysical Research*, 100(E9):19049–19056, 1995.
- [136] W. R. Stockwell. On the HO<sub>2</sub>+HO<sub>2</sub> reaction its misapplication in atmospheric chemistry models. *Journal of Geophysical Research*, 100(D6):11695, 1995.
- [137] D. Stone, L. K. Whalley, and D. E. Heard. Tropospheric OH and HO<sub>2</sub> radicals: field measurements and model comparisons. *Chemical Society Reviews*, 41(19):6348, 2012.
- [138] G. Strazzulla. Cosmic ion bombardment of the icy moons of Jupiter. *Nuclear Instruments and Methods in Physics Research Section B: Beam Interactions with Materials and Atoms*, 269(9):842–851, May 2011.
- [139] I. A. Taub. Transient solvated electron, hydroxyl, and hydroperoxy radicals in pulse-irradiated crystalline ice. *The Journal of Chemical Physics*, 49(6):2499, 1968.
- [140] B. Teolis, J. Shi, and R. Baragiola. Formation, trapping, and ejection of radiolytic O<sub>2</sub> from ion-irradiated water ice studied by sputter depth profiling. *Journal of Chemical Physics*, 130(13):134704–1/8, 2009.

- [141] R. L. Tokar, R. E. Johnson, and M. F. Thomsen. Cassini observations of the thermal plasma in the vicinity of Saturn's main rings and the F and G rings. *Geophysical Research Letters*, 32(14), 2005.
- [142] B. Tremblay, B. Madebne, M. Alikhani, and J. Perchard. The vibrational spectrum of the water trimer: Comparison between anharmonic ab initio calculations and neon matrix infrared data between 11,000 and 90  $\text{cm}^{-1}$ . *Chemical Physics*, 378(1-3):27–36, Dec. 2010.
- [143] G. L. Vaghjiani, A. R. Ravishankara, and N. Cohen. Reactions of OH and OD with  $\text{H}_2\text{O}_2$  and  $\text{D}_2\text{O}_2$ . *The Journal of Physical Chemistry*, 93(23):7833–7837, Nov. 1989.
- [144] M. Van Thiel, E. D. Becker, and G. C. Pimentel. Infrared studies of hydrogen bonding of water by the matrix isolation technique. *The Journal of Chemical Physics*, 27(2):486, 1957.
- [145] S. Vance, J. Harnmeijer, J. Kimura, H. Hussmann, B. deMartin, and J. M. Brown. Hydrothermal systems in small ocean planets. *Astrobiology*, 7(6):987–1005, Dec. 2007.
- [146] A. J. C. Varandas. On the “Ozone Deficit Problem”: What are  $\text{O}_x$  and  $\text{HO}_x$  catalytic cycles for ozone depletion hiding? *ChemPhysChem*, 3(5):433, May 2002.
- [147] R. Vidal, D. Bahr, R. Baragiola, and M. Peters. Oxygen on Ganymede: Laboratory studies. *Science*, 276(5320):1839–42, 1997.
- [148] L. P. Viegas and A. J. C. Varandas.  $\text{HO}_2 + \text{O}_3$  reaction ab initio study and implications in atmospheric chemistry. *Journal of Chemical Theory and Computation*, 6(2):412–420, Feb. 2010.
- [149] D. Vione, V. Maurino, and C. Minero. The atmospheric chemistry of hydrogen peroxide a review. *Annali di Chimica*, 93(4):477–488, 2003.

- [150] R. E. Vogt, A. C. Cummings, T. L. Garrard, N. Gehrels, E. C. Stone, J. H. Trainor, A. W. Schardt, T. F. Conlon, and F. B. McDonald. Voyager 2: Energetic ions and electrons in the Jovian magnetosphere. *Science*, 206(4421):984–987, Nov. 1979.
- [151] J. H. Waite, T. E. Cravens, and W.-H. Ip. Oxygen ions observed near Saturn’s A ring. *Science*, 307(5713):1260–1262, Feb. 2005.
- [152] P. O. Wennberg, R. C. Cohen, R. M. Stimpfle, J. P. Koplów, J. G. Anderson, R. J. Salawitch, D. W. Fahey, E. L. Woodbridge, E. R. Keim, R. S. Gao, C. R. Webster, R. D. May, D. W. Toohey, L. M. Avallone, M. H. Proffitt, M. Loewenstein, J. R. Podolske, K. R. Chan, and S. C. Wofsy. Removal of stratospheric O<sub>3</sub> by radicals: In situ measurements of OH, HO<sub>2</sub>, NO, NO<sub>2</sub>, ClO, and BrO. *Science*, 266(5184):398–404, Oct. 1994.
- [153] E. Whittle, D. Dows, and G. Pimentel. Matrix isolation method for the experimental study of unstable species. *The Journal of Chemical Physics*, 22(11):1943, 1954.
- [154] R. S. Wolff and D. A. Mendis. On the nature of the interaction of the Jovian magnetosphere with the icy Galilean satellites. *Journal of Geophysical Research*, 88(A6):4749–4769, 1983.
- [155] H. Yu and A. Varandas. Ab initio theoretical calculation and potential energy surface for ground-state HO<sub>3</sub>. *Chemical Physics Letters*, 334(1-3):173–178, Feb. 2001.
- [156] W. Zheng, D. Jewitt, and R. I. Kaiser. Formation of hydrogen, oxygen, and hydrogen peroxide in electron-irradiated crystalline water ice. *The Astronomical Journal*, 639:534–548, 2006.
- [157] W. Zheng, D. Jewitt, and R. I. Kaiser. Temperature dependence of the formation of hydrogen, oxygen, and hydrogen peroxide in e-irradiated crystalline water ice. *The Astronomical Journal*, 648:753–761, 2006.

- [158] E.-L. Zins, P. R. Joshi, and L. Krim. Production and isolation of OH radicals in water ice. *Monthly Notices of the Royal Astronomical Society*, 415(4):3107–3112, Aug. 2011.

## Curriculum Vitae

Nhut Do was born in Vietnam and immigrated with his grandparents to the U.S. in 1992. Although leaving at a very young age, he still read and speak Vietnamese fluently. Nhut received a B.S. in chemistry from Virginia Commonwealth University in 2007 and a Ph.D. in chemistry from George Mason University in 2013.